t

CHALMERS
UNIVERSITY OF TECHNOLOGY

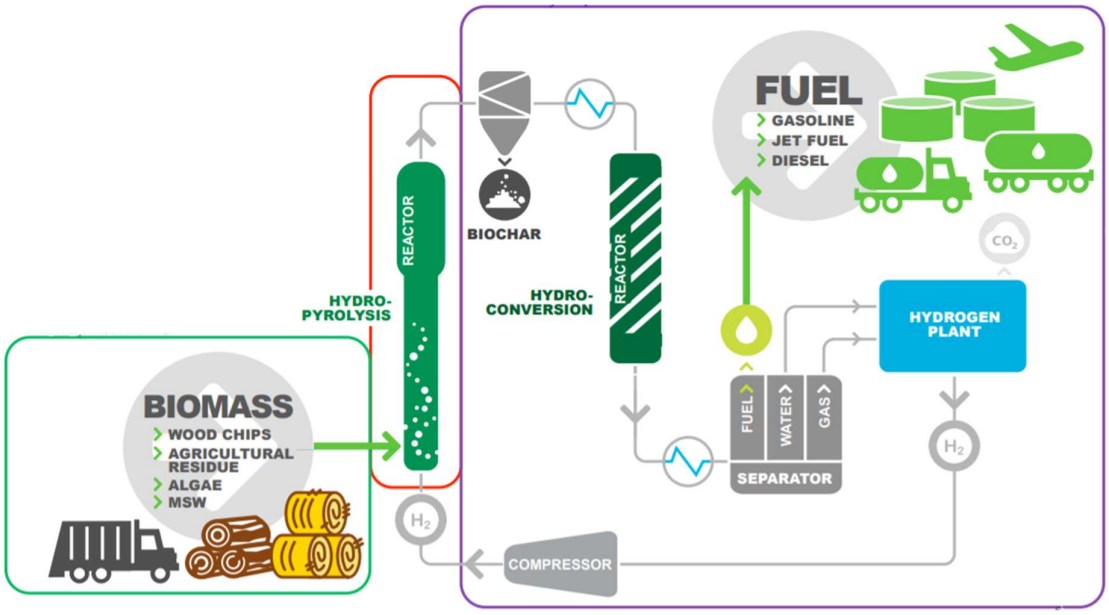

Master's Thesis

Greenhouse gas and techno-economic evaluation of transportation fuels from Integrated Hydropyrolysis and Hydroconversion (IH2)

Gopi Subramaniam
Nordic Master in Innovative Sustainable Energy Engineering

DEPARTMENT OF SPACE, EARTH & ENVIRONMENT
CHALMERS UNIVERSITY OF TECHNOLOGY

Gothenburg, Sweden 2021
www.chalmers.se

MASTER'S THESIS

Error! Reference source not found. Master's Thesis within the *Nordic Master in Innovative Sustainable Energy Engineering* programme

ERROR! REFERENCE SOURCE NOT FOUND.SUPERVISORS:
Elin Svensson, Chalmers Industri Teknik
Shareq Mohd Nazir, KTH Royal Institute of Technology

EXAMINER:
Professor Simon Harvey, Chalmers University of Technology
Professor Mika Jarvinen, Aalto University

Department of Space, Earth and Environment
Division of Energy Technology
CHALMERS UNIVERSITY OF TECHNOLOGY
Göteborg, Sweden 2021

Greenhouse gas and techno-economic evaluation of transportation fuels from Integrated Hydropyrolysis and Hydroconversion (IH2)
Master's Thesis within the *Nordic Master in Innovative Sustainable Energy Engineering* programme
GOPI SUBRAMANIAM

Department of Energy and Environment
Division of Energy Technology
Chalmers University of Technology
SE-412 96 Göteborg
Sweden
Telephone: + 46 (0)31-772 1000

Cover: Schematic representing IH2 process, as depicted by CRI Catalyst Co. (https://www.svebio.se/app/uploads/2018/09/6.Alan_Del-Paggio.pdf)

Chalmers digitaltryck
Göteborg, Sweden 2021

Greenhouse gas and techno-economic evaluation of transportation fuels from Integrated Hydropyrolysis and Hydroconversion (IH2)
Master's Thesis within the *Nordic Master in Innovative Sustainable Energy Engineering* programme
GOPI SUBRAMANIAM
Department of Energy and Environment
Division of Energy Technology
Chalmers University of Technology

Abstract

The aim of this thesis was to evaluate the production of gasoline and diesel using woody biomass feedstock via the Integrated Hydropyrolysis and Hydroconversion (IH2) technology from a technical, economic and greenhouse gas (GHG) emissions perspective.

The methodology was first to model the IH2 process based on published experimental data via a combination of mass and energy balances and Aspen Plus computer simulation. The results indicated a liquid hydrocarbon yield of 26% on a dry ash free feed basis and an overall system efficiency of 60%.

The results from the process modelling were then used to build up an operating expenditure (OPEX) estimate for an IH2 plant based on two future energy market price scenarios, which then allowed for an estimation of the capital expenditure that could be supported while maintaining a reasonable operating margin. The results showed that OPEX was primarily driven by the biomass feed price, and to a much lesser extent the price of wholesale grid electricity and external refinery final processing costs. Furthermore, the capital expenditure that could be supported was shown to be high compared to previously published capital cost estimates for the IH2 process. This result was shown in scenarios both with and without a supportive policy environment for biofuels.

Finally, a well-to-wheel GHG emissions balance was estimated. The relative emissions savings compared to the corresponding fossil transportation fuels were primarily dependent on the assumed marginal user of biomass and if the biomass was considered a limited resource. If biomass is a limited resource and the marginal user a coal fired power plant, the emissions savings were approximately 38%, while the savings were greater than 97% if biomass was not considered a limited resource.

Acknowledgements

First and foremost, I would like to thank my supervisors Shareq Nazir and Elin Svensson. Shareq provided valuable guidance on process modelling and the usage of Aspen Plus, while Elin was always available to share her considerable experience and constructive feedback on the overall direction, content, and purpose of this thesis.

I would also like to express gratitude to all the people involved in the ISEE program at both Aalto University and Chalmers University of Technology for giving me the opportunity to pursue my passion in sustainable energy. The last two years have been incredibly rewarding and life changing.

Table of Contents

List of Tables

List of Figures

List of Abbreviations

a.f.	As Fed Basis
a.r.	As Received Basis
CAPEX	Capital Expenses
CCS	Carbon Capture and Storage
d.a.f.	Dry Ash Free Basis
d.b.	Dry Basis
ENPAC	The Energy Price and Carbon Balance Scenarios
FOAK	First-of-a-Kind
FPO	Fast Pyrolysis Oil
FTD/G	Fischer-Tropsch Diesel/Gasoline
FTR	Fired Tubular Reformer
HC	Hydrocarbon
HHV	Higher Heating Value
HRSG	Heat Recovery Steam Generator
LCA	Life Cycle Analysis
LHV	Lower Heating Value
LCOE	Levelized Cost of Electricity
MAT	Minimum Approach Temperature
NGCC	Natural Gas Combined Cycle
NOAK	N^{th}-of-a-Kind
OPEX	Operating Expenses
PSA	Pressure Swing Adsorber
IH2	Integrated Hydropyrolysis and Hydroconversion
NCG	Non-Condensable Gases
SC	Steam to Carbon ratio (molar)
SMR	Steam Methane Reforming
TCI	Total Capital Invested
WGS	Water-Gas Shift
WHSV	Weight Hourly Space Velocity
WTP	Willingness to Pay

1. Introduction

1.1. Background

Sweden has set an ambitious target of becoming a net-zero emitter of greenhouse gas (GHG) emissions by 2045. Within this framework, GHG emissions specific to the domestic transport sector, excluding aviation, are to be reduced by 70% from 2010 baseline levels by 2030 [1]. Sweden has good availability of forestry and agricultural residues that can be used as feedstocks to produce renewable transportation fuels that could be a promising part of the solution towards this goal. Biofuels currently account for 19.5%, or 16 TWh/a, of all Swedish transportation energy requirements [2]. By 2045, it is estimated that renewable biofuels could supply up to 38 TWh/a for transportation needs, indicating significant scope for increasing supply [3].

Developing hydrocarbon (HC) based drop-in biofuels such as renewable gasoline and diesel has the advantage that such fuels can be used in existing distribution networks and are compatible with much of the existing vehicle fleet, and already account for 12.3% (HVO) of Swedish transportation fuel use on an energy basis [2]. This is in contrast with other more common biofuels that are instead blended into fossil fuels, such as ethanol or FAME (i.e Fatty Acid Methyl Esther). Indeed, drop-in fuels from biomass waste feedstocks have been identified as a priority by the Swedish Energy Agency [4].

One common process route to produce drop-in biofuels is pyrolysis where biomass is thermochemically broken down in the absence of oxygen. However the bio-oil that results from this process needs to be upgraded using hydrogen, in a process called hydrodeoxygenation (HDO), to remove oxygen and stabilize the oil, and then refined to produce the required cuts of bio-fuels (e.g. gasoline, kerosene, diesel etc.).

This work was conducted within the framework of a collaborative project between KTH and Chalmers University of Technology focussed on developing a techno-environmental-economic assessment of four pyrolysis-HDO integrated process routes, with a separate downstream refining step to produce drop-in transportation fuels using wood fuel feedstocks available in Sweden. The project is funded by the Swedish Energy Agency and f3, which is the Swedish knowledge centre for renewable transportation fuels, with Cortus Energy AB as the industrial partner.

The four process routes to be investigated are; 1) Pyrolysis-HDO with hydrogen from electrolysis; 2) Pyrolysis-HDO with hydrogen from biomass gasification (with and without carbon capture and storage (CCS); 3) Pyrolysis-HDO with hydrogen from reforming of natural gas (NG) with CCS; 4) Integrated hydropyrolysis and hydroconversion (IH2). Figure 1 shows a representative schematic of these different processes.

In the first three process pathways, biomass is pyrolyzed to produce fast pyrolysis oil (FPO) and then hydrotreated to produce a fungible petrol-diesel blend. The differences between the three are the manner in which hydrogen for hydrotreatment is obtained. In the first process route, water goes through electrolysis powered by renewable energy to produce hydrogen. In the second route, additional biomass feed is gasified and the resulting producer gas is upgraded to produce hydrogen. In the third route hydrogen is produced in what is currently the most conventional technology via steam-methane reforming (SMR) of natural gas. The fourth route on the other hand is a very different technology that pyrolyzes the feed in a pressurized hydrogen environment, where the hydrogen is produced endogenously within the process. In this process hydropyrolysis is integrated with hydroconversion step via two consecutive reactors. This process is described in more detail below.

What is unique about this project is that, within the context of Sweden, it investigates the integration of various hydrogen generation technologies for HDO within the biofuel production process itself, and not at the refinery which is typical of some other studies [5], [6].

The overall objective of the project is to reinforce the publicly available knowledge base of advanced drop-in biofuel production processes and how these processes could be integrated into existing infrastructure.

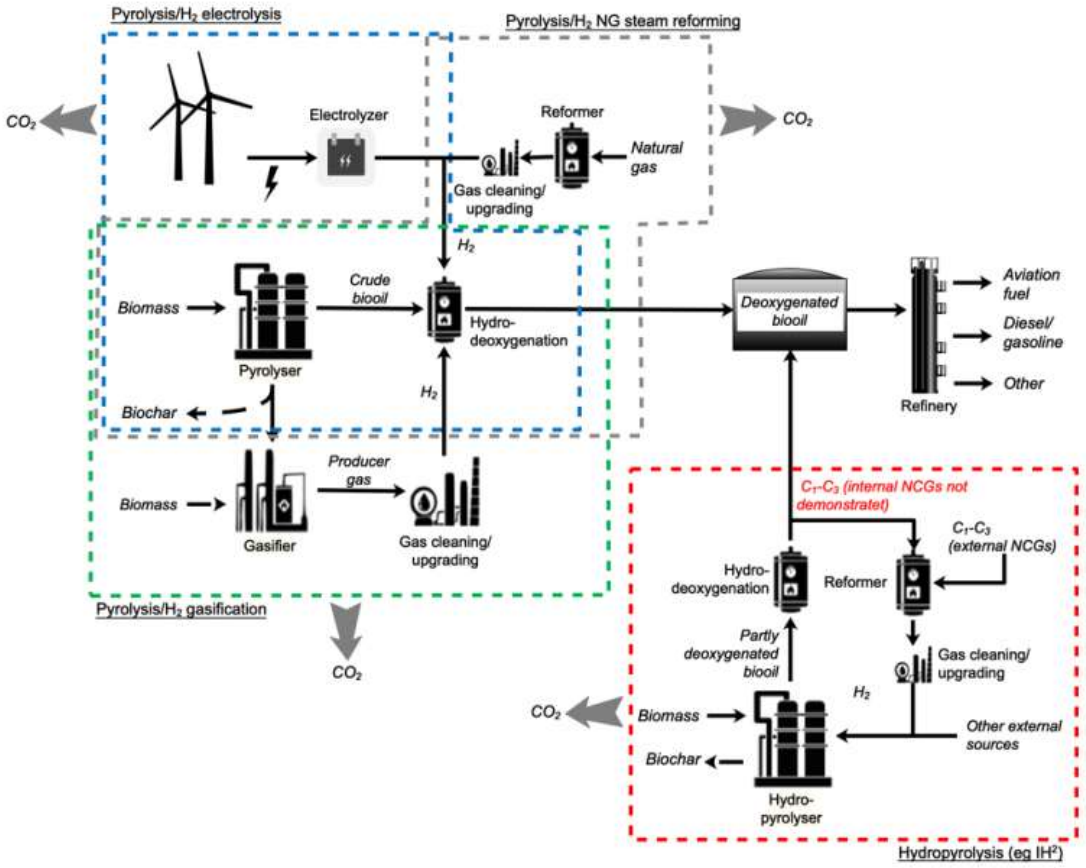

Figure 1: Process flow schematic of scenarios to be investigated[1]
IH2 is the focus of this thesis

The scope of this thesis is a subset of this larger project. Specifically, this thesis develops a process model of the IH2 process and uses various metrics to evaluate its technical performance. Following this, the processes' economic viability and GHG emissions are also evaluated. The technical, economic and emissions evaluation metrics will then form the framework by which the other three processes, modelled by KTH, will be subsequently evaluated and then compared against each other.

[1] Note that the deoxygenated bio-oil from the IH2 process may not necessarily have the same properties as the products from the other three processes as implied in the figure. Further the dashed lines should not be taken as system boundaries for evaluation and comparison. The system boundary of the IH2 process for this study is detailed in section 2

1.2. Previous Related Work

The primary basis of this work stems from the various published papers and patents issued by the IH2 technology developer, the Gas Technology Institute (GTI), from 2010 onwards. The published papers covered the initial bench scale (0.45 kg/hr) and subsequent lab scale (50 kg/day) experimental data which formed a proof of concept for the IH2 process [7]–[10]. This was followed by a techno-economic analysis[11] and Life Cycle Analysis (LCA)[12] to further justify the merits of the process. Since then, other works related to the IH2 process and comparisons with other biofuel production processes have also been carried out.

In terms of experimental data, other lab scale experiments have attempted to determine the effect of changing key process parameters (e.g. pressure, temperature, catalyst type determine the effect on the product composition and quality [13]–[16]. The findings in these papers shed further light into the various hydrocarbon species that are formed via hydropyrolysis, as well as providing a more detailed characterization of the by-product char.

Process modelling of the IH2 process has also been done by other researchers by conducting a thermodynamic and pinch analysis for flow sheet optimization [17], and incorporation of CO_2 capture [18]. This study relied on the latter for much of the calculation methodology for mass balances and hydrogen rate requirements as detailed in Section 3.1. To model the non-condensable gas (NCG) reformation process however, this study built on previous work on natural gas reformation modelling using Aspen Plus [19]–[21] as described in Section 3.1.2.

Techno-economic and greenhouse gas (GHG) emissions analyses of the IH2 process have also been performed by other researchers[18], [22] finding their results to be largely consistent with the technology developer's original estimate. Comparison studies with other biofuel production processes [5], [6] within the context of integration of a biofuel production facility within a pulp mill, finds the IH2 process comparing favourably to the other biofuel production processes.

1.3. Scope and Objectives of Thesis

The scope of this study involves completing a technical, economic and GHG emissions evaluation of the IH2 process with any potential refining requirements for the produced biofuel included within the system boundary in order to produce a saleable commodity fuel product. The objectives can hence be broken down as follows:

- Develop a process model for the IH2 process, using process simulation software or other suitable modelling tools, depending on the quality of available published experimental data
- Develop technical metrics by which to evaluate the IH2 processes' performance and compare those results to published literature data
- Establish future scenarios with energy price and emissions data based on consistent energy carrier substitution principles to be used for economic and GHG emissions evaluations
- Assess the economic viability and GHG emissions reduction potential of the IH2 process

The technical, economic and GHG emissions metrics used to evaluate the IH2 process should also be meaningful and applicable to the other three process routes and provide a valid basis for an inter-process comparison of all four process routes in a subsequent study.

Ultimately this will help to answer the larger question of whether biofuel production via fast pyrolysis with integrated HDO using wood fuel feedstock could be a cost competitive

proposition in the Swedish context while providing significant reductions in GHG emissions in the Swedish transportation sector.

1.4. Limitations

The experimental data used for this study is from the original paper published by the technology developer. Since then other lab scale experiments have attempted to investigate various aspects of the IH2 process as discussed above in Section 1.2, but not at any larger scale. Hence the performance of an IH2 commercial facility cannot be confidently ascertained from published literature.

The IH2 process model in this study focuses on the most important parts of the process such as hydropyrolysis, hydroconversion and hydrogen production. Within the hydropyrolysis and hydrotreatment process, a black box energy and mass balance is performed rather than a more detailed process simulation model, since chemical reaction kinetic models are not available in literature presently. Hence the ability to analyse the effect of changes to process parameters such as temperature, pressure or feed characteristics is not possible. This is in contrast to non-catalytic fast pyrolysis where reaction kinetic models have been developed [23].

The hydrogen production system is simulated with Aspen Plus based on literature models of the SMR process, and hence has not been optimized to the specific NCG composition from the IH2 process. To be able to do this would require specialist knowledge only available to manufacturers of such packaged reformer systems and hence falls outside the scope of this thesis. Further the steam generation system within the hydrogen production system is modelled very simply without optimizing steam property data or heat recovery. Hence there is significant scope for further improvements to the model.

Other key processes such as feed handling, pyrolysis product phase separation and refinery operations are not modelled in detail and instead have simplified assumptions to account for energy usage and associated costs. Auxiliary systems not directly related to the efficiency and performance metrics of the process such as wastewater treatment and NCG gas pre-treatment are not modelled, although cost information of these systems is incorporated into the overall operational cost calculations of this study.

From an economic perspective, only the IH2 operating costs are modelled as part of this thesis' scope. The source of the operating cost estimate relies heavily on the technology developer's original estimate which are more than a decade old and have likely gone through considerable refinement since then with the many thousands of hours of operations of their demonstration plant in India (see Section 2.1). However, data from this demonstration facility is not published. Capital cost estimates are not independently developed in this study, using instead the two existing estimates from literature inflated to current prices. Both these estimates must be viewed with caution as they use a factored estimation methodology since the technology does not yet have a commercial facility from which to base a more detailed capital cost estimate.

The prices and emission factors for future scenarios used in the economic and GHG emissions analysis have been generated using the ENPAC tool (refer to Section 3.3.1 for description). The inputs defining these scenarios and the models inherent in the tool are based on many different assumptions such as policy support systems, structures of electricity and biomass fuel markets that are specific to a Northern European context.

Finally, this study does not include a comparison between the four process routes as the results from the modelling of the three pyrolysis process routes by KTH were not ready in time for the completion of this study. Hence some potentially interesting findings and conclusions from the inter-process comparisons will only be revealed in a later publication as part of this larger project.

2. The IH2 Process

2.1. Hydropyrolysis vs Pyrolysis

Biomass fast pyrolysis is a thermochemical pathway to convert waste biomass feedstocks, such as forestry and agricultural wastes, into bio-oil. The bio-oil can then be subsequently upgraded into drop-in renewable biofuels which could leverage existing refining, distribution, and vehicle fleet infrastructure to provide for transportation needs in areas that are difficult to electrify [6], [24].

The process involves the thermal decomposition of biomass at intermediate temperatures (~400-600°C), high heat transfer rates and in the absence of oxygen. The products of this process are char, bio-oil and NCGs. The most valuable product, bio-oil, needs to be upgraded before it can be used as a fuel. Bio-oil is a challenging intermediate product that has high oxygen content (~40%), low heating value, high corrosivity (Total Acid Number TAN ~100-200), is chemically unstable over short time spans, and generally immiscible with petroleum fractions. The problematic aspects of bio-oil are largely a result of the high proportion of oxygenated compounds present. Hydroconversion has been demonstrated to remove the oxygen in the bio-oil but this also presents various challenges. These include low weight hourly space velocities (WHSV, 0.1-0.2 $kg_{biomass}/kg_{catalyst}/hr$), high hydrogen partial pressures (up to ~170 bar) and different operating pressure to the upstream pyrolysis process, the addition of 3-5 wt% hydrogen on a bio-oil feed basis thereby requiring an external source of hydrogen, specialty steels to handle the corrosivity of the bio-oil feed, and reactor plugging issues due to coking and polymerization. These factors make it challenging and expensive to handle, transport and upgrade [25]–[28].

One process pathway that has been developed to overcome these issues is Integrated Hydropyrolysis and Hydroconversion (IH2). This technology was developed and patented by GTI and licensed to Royal Dutch Shell for exclusive worldwide deployment. Shell subsequently built and is currently operating a demonstration plant capable of producing up to 5 tonnes/day of fungible gasoline/diesel blend using various biomass feedstocks [29]. There have also been recent reports of license agreements for a commercial scale plant in Norway thereby indicating a potentially high Technological Readiness Level (TRL) [30].

IH2 is reported to have several advantages over conventional pyrolysis-HDO process pathway variants. It can process a wide variety of waste biomass such as woody lignocellulosic waste, agricultural waste (e.g. corn stover, bagasse, cotton stalks, corn cobs, castor stalks, sugarcane tops etc.), algae and even waste plastic. Furthermore, IH2 is a self-sustaining process in which the heat required for pyrolysis is supplied by the exothermic deoxygenation process. The hydrogen requirements are met entirely by steam reforming the light NCGs (C1-C3) that are produced as part of the hydropyrolysis process. Water requirements for reforming are also produced internally by the process. Hence it is not necessary to severely dry the feed since feed water content is advantageous to in-situ H_2 formation through the water-gas shift reaction. Process temperatures and pressures are moderate (i.e. 20-35bar and 350-480°C), and both hydropyrolysis and hydrotreatment reactors operate at the same pressure. The main outputs of the process are biochar and a fungible gasoline/diesel blend stock that is almost completely deoxygenated, has a high heating value, low acidity, and is compatible with existing refinery operations. Other valuable output streams include steam (for reforming and other uses), ammonia and ammonium sulphate [31].

2.2. IH2 Process Description

IH2 is a two-stage, catalytic fast hydropyrolysis process integrated with a downstream hydrotreatment reactor to produce a fungible gasoline/diesel blendstock using various biomass and plastic waste feedstocks. Feed and hydrogen are introduced into a fluidized bed reactor at between 20-35 bar and temperatures between 350-500°C. The feed is thermo-catalytically converted to low oxygen content HC vapours and char, while the oxygen is removed as water and CO_x. Unlike conventional fast pyrolysis, catalytic hydro-pyrolysis minimizes undesirable coking reactions and acid catalysed polymerization and aromatization. Hence the catalyst cokes very slowly over many months and requires no regeneration [7]. The operating parameters of hydrogen fluidization velocity, catalyst bulk density and size, and biomass bulk density and size are chosen to ensure that the catalyst remains in the reactor while the char is entrained within the fluidizing hydrogen [32]. Hence hydrogen gas serves as both a fluidizing and deoxygenation agent. In the fluidized bed reactor, the catalyst itself serves as bed material. The catalyst is a sulphided catalyst with one or more metals from nickel, cobalt, molybdenum, or tungsten embedded on a metal oxide support such as alumina [33]. Although feed devolatilization is endothermic, catalytic hydro-deoxygenation is exothermic resulting in the hydropyrolysis reaction being net exothermic [34].

In conventional pyrolysis the removal of char from gas phase products can be technically challenging. The high oxygen and free radical content of the vapours form a pitch-like material when coming into contact with char particles, thus plugging up any filters used to remove char. In hydropyrolysis the free radicals are stabilized resulting in much easier char separation from the gas stream [8]. Typical char and catalyst fines removal methods in the IH2 process are cyclones in combination with hot gas filters, or alternatively bubbling the first stage reactor vapours through a recirculating high boiling point and fully saturated cut of the polished HC product liquid. The latter method has the added advantage of cooling the vapours for the subsequent second stage hydroconversion reactor while avoiding any filter plugging issues [33].

The second stage hydroconversion reactor is a fixed bed reactor. The catalyst material is similar to the first stage reactor. This reactor operates at the same pressure, but slightly lower temperature (260-430°C) compared to the first stage reactor [33]. The purpose of the second stage reactor is to remove any remaining hetero atoms such as nitrogen and sulphur from the HCs. The main components of the product stream from the second stage hydroconversion reactor include hydrogen, condensable and non-condensable HCs, water, CO_x, hydrogen sulphide and ammonia [31].

These gases are then put through a series of high pressure and low-pressure separator-condensers where the water, condensable HCs and other gases are separated. The condensable HCs at this point have a low TAN of <1 as well as very low oxygen, nitrogen and sulphur content. This product is of sufficient quality to be used as gasoline and diesel blend-stocks for further downstream processing. The water is stripped of ammonia and hydrogen sulphide, and along with the non-condensable HCs and CO_x, is sent to a steam reformer [31]. Part of the non-condensable gases are combusted to provide heat to turn the water to steam and raise the temperature for the reforming process. A Pressure Swing Adsorber (PSA) is a final step to extract the hydrogen as the product from the reforming process to be circulated to the first stage reactor, with CO_2 from the combustion of biogenic matter being released to atmosphere [33]. An important claim made by the technology developers, which represents a big advantage over other fast pyrolysis processes is that all the energy requirements for reforming and steam production, water requirements for steam, and electricity requirements

for the plant can be satisfied from reforming the non-condensable gases produced from the two reactors. This claim will be investigated in this study.

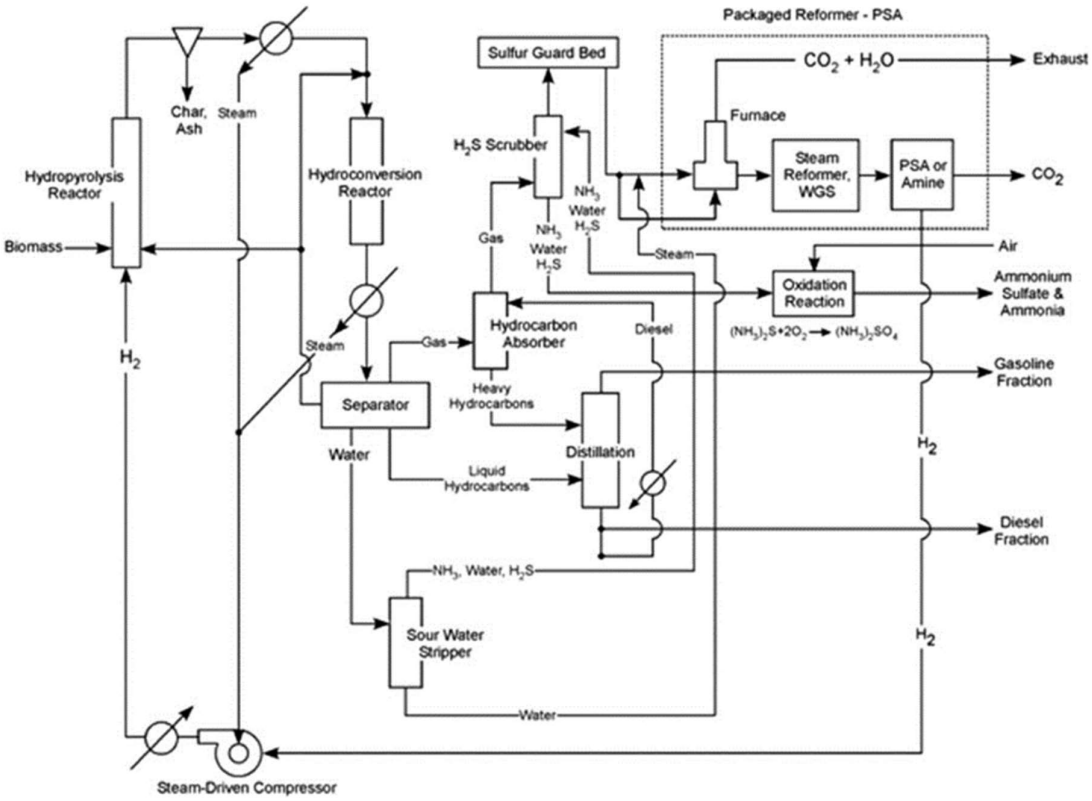

Figure 2: Process flow schematic of IH2 process by the technology developers, GTI [11]

There are a few important factors that determine the IH2 process' overall operating temperature and pressure. Higher pressures favour hydrodeoxygenation, producing more liquid HCs but also resulting in more water, and hence higher hydrogen consumption. Lower pressure favours decarboxylation which is undesirable since carbon is lost as CO_2. Hence the pressure level is a trade-off to keep hydrodeoxygenation and decarboxylation in balance. Higher temperatures on the other hand leads to higher light end (i.e. C1-C3) gas yields, which forms the feedstock for the reformation process to produce makeup hydrogen, at the expense of char. However, operating temperature is limited by catalyst operating limits, and the fact that excessively high temperatures can inhibit saturation reactions and promote coking. Hence, should the process fail to produce sufficient hydrogen for internal consumption, the temperature can be increased as a corrective measure within the aforementioned limits[14], [15].

Liquid product yields can range from 25-30% with a molar Hydrogen to Carbon ratio of between 1.4 for woody biomass feedstocks and up to 1.7 for algae [31].

3. Methodology

The following section will broadly outline the methods, tools and calculations performed to achieve the objectives of this study. It is separated into two broad areas; process modelling and economic and GHG emissions evaluation.

The system boundary by which the process modelling, economic and GHG emissions evaluations were conducted is shown in Figure 3. HDO is, as a feature of the IH2 process, already integrated within the IH2 plant. This is in contrast with the other three process routes where an intermediate fast pyrolysis bio-oil is produced which must then go through a separate HDO process. The system boundary also covers any potential refinery operations for the deoxygenated bio-oil product that may be required to produce a consumer fuel product.

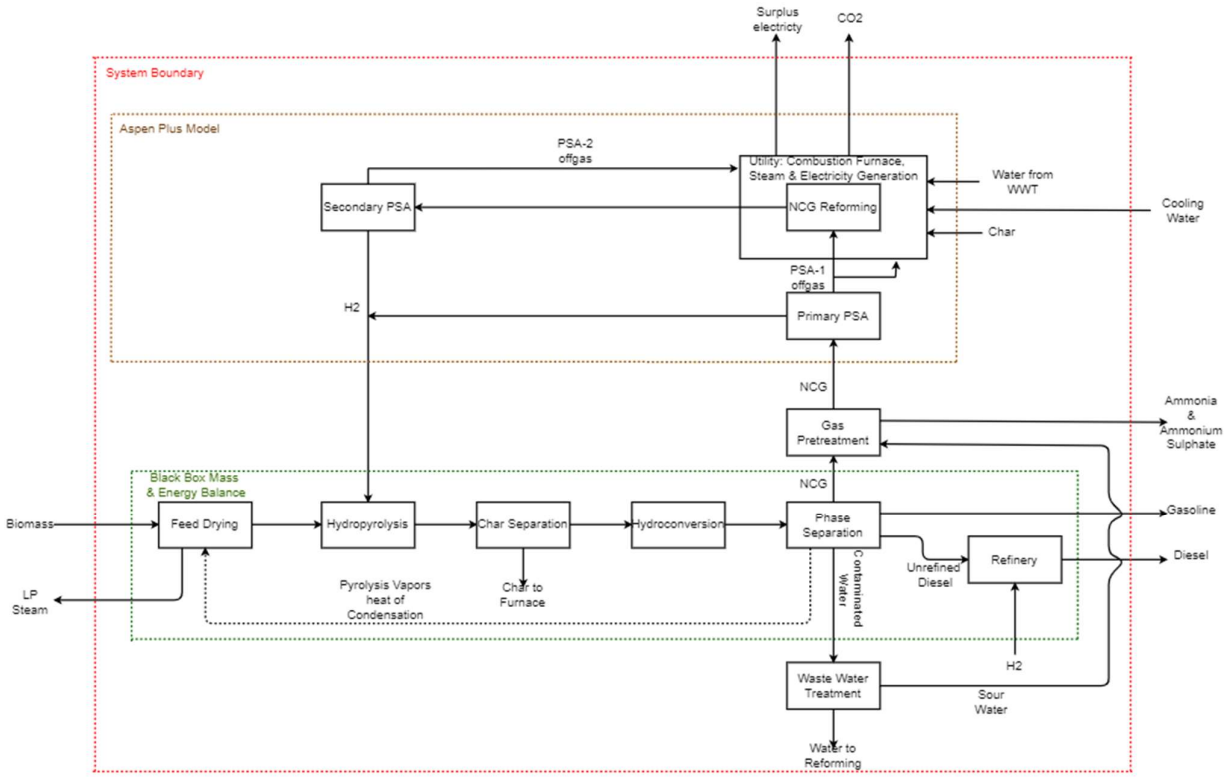

Figure 3: IH2 process flowsheet as modelled in this study

3.1. IH2 Process Modelling

The following section describes how the IH2 process was modelled using a combination of energy and mass balances and Aspen Plus. The degree to which modelling was possible was based on the availability of published experimental results and simulation models. The modelling work can be broken down into three interconnected processes. The first is the hydropyrolysis and hydrotreatment which forms the heart of the IH2 process where the fungible gasoline/diesel product is formed. The second is the reforming of the NCGs to produce hydrogen. The third is all the auxiliary systems that support the IH2 process.

3.1.1. Hydropyrolysis and Hydroconversion

There was no published literature on the kinetics of the hydropyrolysis and subsequent hydroconversion process of biomass that could be found to construct a simulation model in Aspen Plus. Hence this part of the process involved only a mass and energy balance that would become inputs to other downstream and upstream processes.

The basis of the mass balance comes from the original IH2 experimental data set from experiments run in a 0.45kg/hr pilot plant. The data set features bench scale experimental data using various feedstocks such mixed wood, maple, lemna, algae, bagasse and corn stover. The experiments were run at different temperatures, using different catalysts as well as with just hydropyrolysis without hydroconversion and then again with both hydropyrolysis and hydroconversion steps. The experiments were run over time frames of 2-18 hours on a semi-continuous basis [7], [10].

There can be some confidence in the repeatability of these experimental results since subsequent experimental data from a larger 2kg/hr continuous pilot plant showed similar results [8].

This study used a ‘mixed wood’ experimental data subset. Mixed wood from the pilot plant experiments was defined as a mixed feed of 68% hardwood and 32% softwood representing a woody biomass feedstock blend typically available in the midwestern US. Among all the experimental feedstocks this was judged the closest wood waste feedstocks that could feasibly be found in Sweden. Initially a mass balance was attempted downstream of the hydropyrolysis step (i.e. data set from experiment 3/9) and then again downstream of the hydroconversion step (i.e. data set from experiment 8/23). Both these data sets used the same hydropyrolysis catalyst, temperature and pressure set points. However, without more information it was not possible to reconcile the results consistently to accurately depict the reaction developments between the two reactors. Hence the hydropyrolysis and hydroconversion steps were treated as a single black box over which a mass balance was calculated. The input experimental data used is shown in the tables below.

Table 1: Mixed wood ultimate analysis

Mixed Wood Ultimate Analysis				
	As fed (a.f.)	Dry basis (d.b.)	Dry ash free (d.a.f.)	As received (a.r.)
Moisture	5.60%	-	-	30.00%
C	46.92%	49.70%	49.95%	34.79%
H	5.48%	5.80%	5.83%	4.06%
O	41.40%	43.86%	44.08%	30.70%
N	0.10%	0.11%	0.11%	0.08%
S	0.03%	0.03%	0.03%	0.02%
Ash	0.47%	0.50%	-	0.35%

Experimental data is shown in the 'as fed' column while the other columns are calculated from this. It is assumed that the feed is delivered to the plant with 30% moisture and is dried to 5.6%, which is the moisture content of the feed used in the experimental data.

Table 2: Experimental product compositional breakdown

Mixed Wood 8/23 Results (d.a.f. basis)		
Temperature (°C)	389	
Pressure (bar)	22.4	
Catalyst (Hpyr/HDO)	4211/4202	
Run time (h)	3.3	
	Original data	**Adjusted data**
Experimental Overall Yield		
C recovery	101.00%	101.00%
CO, wt% d.a.f.	6.50%	6.50%
CO2, wt% d.a.f.	7.40%	7.40%
C1-C3, wt% d.a.f.	14.50%	14.50%
Liquid, wt% d.a.f.	25.80%	25.80%
Char, wt% d.a.f.	13.40%	13.40%
Water, wt% d.a.f.	37.00%	37.00%
H2 added, wt% d.a.f.	-4.60%	-4.60%
Hydro-Carbon Liquid Product Analysis		
% O, wt%	<2.2%	1%
% C, wt%	85.25%	87.22%
% H, wt%	11.45%	11.72%
% N, wt%	0.06%	0.032%
% S, wt%	0.01%	0.0052%
Density	0.86	0.86
% Gasoline	66%	66%
% Diesel	34%	34%
TAN	0.33	0.33
RON	86	86
H:C Molar Ratio	1.61	1.60
Hydro-Carbon Gas Composition		
Methane, wt%	25.70%	25.70%
Ethane, wt%	46.10%	46.10%
Propane, wt%	28.20%	28.20%
Ethylene, wt%	-	-
Propylene, wt%	-	-
Wastewater Analysis		
pH	8	8
% N, wt%	0.13%	0.13%
% C, wt%	0.19%	0.19%
% S, wt%	0.01%	0.01%
% NH3, wt%	0.13%	0.13%

Table 2 shows how the original experimental data was adjusted for the purposes of the mass balance. The adjustments were in the liquid product specifications where the oxygen, nitrogen and sulphur contents were adjusted to match liquid product analysis data, shown in Table 3 below, while the hydrogen and carbon values were normalized. The liquid product data represents part of the product specification from the IH2 process from which the refinery requirements are determined as detailed in Section 3.1.4. Hence for consistency the experimental data in Table 2 was adjusted.

Table 3: Liquid product analysis from mixed fuel feedstock

Liquid Product Analysis		
	Gasoline	Diesel
Oxygen, Wt%	1%	1%
TAN	<0.6	<0.6
RON	87	-
Cetane	-	22
H/C (molar)	1.7	1.3
H/C (wt)	0.14	0.11
S, ppm Wt	52	52
N, ppm Wt	162	634
Paraffin	19%	-
Napthene	44%	-
Aromatic	37%	-

With the data above, the distribution of elements after hydroconversion can be determined. A nominal 'as fed' feed rate of 1kg/s was used.

The hydrogen flow rate was determined using the same methodology as Meerman & Larson [10]. Hydrogen serves three functions in this process: as a reactant, a fluidizing agent, and a thermal regulator since the reactions are exothermic. The largest of these three calculated values was used as the hydrogen flow rate. A brief description of how each of these three values was calculated is described below, while the detailed calculations can be found in Appendix A - H2 Flow Rate Calculation for Hydropyrolysis

Hydrogen as a reactant can be determined directly from the experimental data as per Table 2, which results in a required flow rate of 0.046 kg H_2/$kg_{biomass\ d.a.f.}$ This value is necessarily the lowest of the three since the hydrogen flow rates required for fluidization and heat transport would have to include the reactant amount. This is because the reactant hydrogen is 'consumed' during the hydropyrolysis process and hence plays no part in thermal regulation or fluidization.

For fluidization, the minimum fluidization velocity was calculated, from which a safety margin of 2 was applied for the design fluidization velocity. The key data points used for these calculations were the reported WHSV of hydropyrolysis from experimental data [7], and catalyst physical characteristics from Meerman & Larson [18]. The minimum fluidization velocity was then calculated based on correlations developed by Kunii & Levenspiel [35]. As mentioned previously, the catalyst itself is the fluidization medium in the IH2 process and is kept in the reactor by virtue of it having a higher density than the feed. The hydrogen required for fluidization plus the amount required for reaction was calculated at 0.14 kg_{H2}/$kg_{biomass\ d.a.f.}$

For thermal regulation, an energy balance had to be solved across the two reactors to obtain the required hydrogen flow rate. The feed is first dried from 30% as received moisture to 5.6% as fed moisture using 1.2bar superheated steam (refer to Section 3.1.3) and hence the feed

is assumed to be at 104ºC when entering the reactor. Hydrogen gas enters the reactor after compression at 41ºC, which is the value obtained from the NCG reforming Aspen Plus model as described in Section 3.1.2. All pyrolysis products exiting the reactor are at 389 ºC as per reported experimental conditions in Table 2. It is assumed that all the catalyst stays in the bed and that the reactor is adiabatic and operating at steady state. Then the energy balance reduces to the thermal and chemical energy of the incoming reactants equalling the thermal and chemical energy of the outgoing products:

$$Chemical\ Energy\ (MW) = \sum(\dot{m}_i \Delta H_c)$$
$$Thermal\ Energy\ (MW) = \sum\left(\dot{m}_i\ c_p \Delta T\right)$$

where $\dot{m}$ represents mass flow rate with the subscript 'i' denoting different compounds. Chemical energy is the energy released from the hydropyrolysis reaction and this is the energy that is assumed to provide heat to all the products and raise the exiting flow temperature to 389 ºC. The heat of combustion, ΔH_c, is used to estimate chemical energy. Both heat capacities, c_p, and the heat of combustion were either obtained from literature or directly from Aspen Plus.

For non-conventional heterogenous compounds, the heat of combustion was estimated using the following correlation, inputting elemental weight fractions of the compound as follows [36]:

$$\Delta H_c(MJ/kg) = 34.91C + 117.83H - 10.34O - 1.51N + 10.05S - 2.11Ash \quad \textbf{Eq\# 1}$$

From the above the only unknown is the hydrogen flow rate. Then solving for this, and including the hydrogen required for the reaction, results in a flow rate of 0.230 kg H_2/$kg_{biomass,d.a.f.}$ .This value, being the largest of the three values, is hence used in the Aspen Plus NCG reforming model since it satisfies all the three aforementioned functions of hydrogen for hydropyrolysis.

3.1.2. NCG Reforming

The NCG reforming process has the primary function of producing enough makeup hydrogen to replace the reactant hydrogen consumed in the hydropyrolysis and hydroconversion processes. At the same time, this process also needs to generate sufficient heat to support the endothermic gas reformer and produce sufficient steam which is an input to the reformer along with the NCG. An additional objective would be to generate sufficient excess heat over and above this basic requirement to generate electricity at least for internal plant uses. An Aspen model of this process was constructed to see if it could achieve these things without requiring exogenous utility supply as claimed by the IH2 process technology developers [31].

The reforming process flow sheet, including the gas combustion and steam generation processes, were modelled based on similar published literature on natural gas reforming process modelling [19]–[21]. The flow sheet was adapted where necessary to suit the specifics of the IH2 process as described below. A simplified version of this flowsheet is presented in Figure 4.

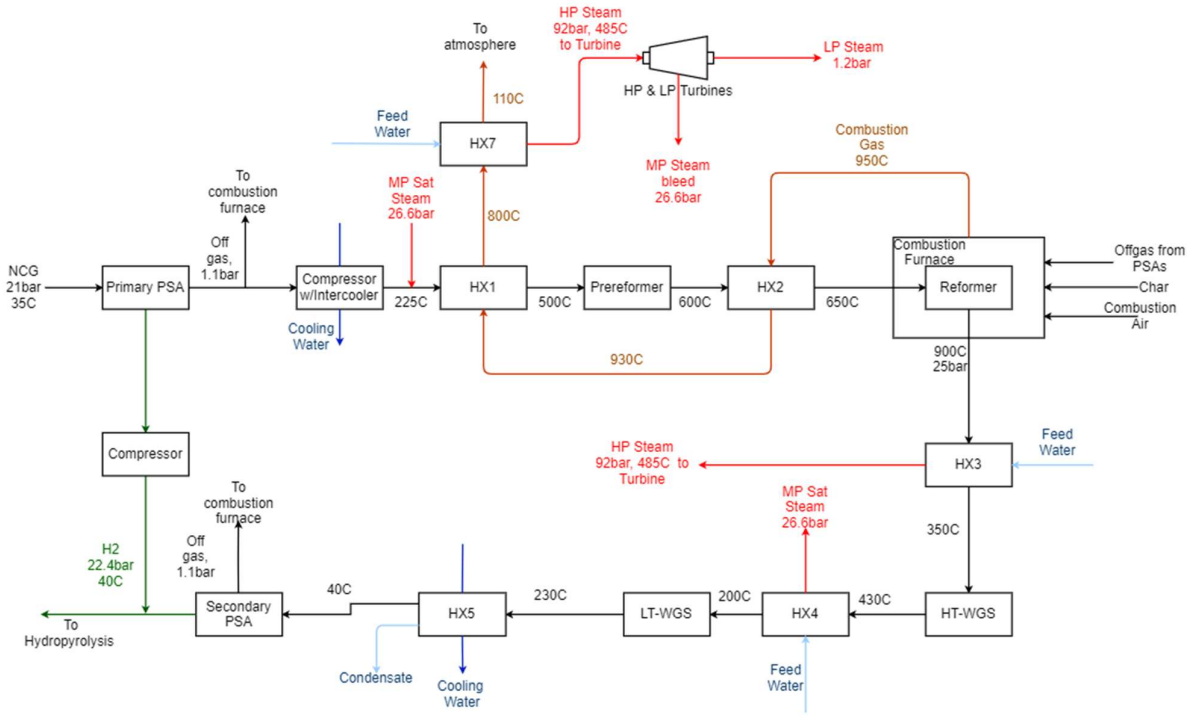

Figure 4: NCG reforming flowsheet for Aspen Plus modelling

The incoming NCG composition is based on the mass balance of the preceding hydropyrolysis and hydrogenation section. The experimental IH2 data was based on a reactor temperature of 389°C operating at 22.4bar. It is assumed that the NCGs enter the reforming process at 21bar, due to pressure drops across the reactors and associated equipment, and 35°C from product stream cooling to condense out water and HC liquids.

The incoming NCGs first go through a primary PSA where most of the excess hydrogen is separated and sent back to the hydropyrolysis reactor. This reduces the gas flow load into the reforming process train thereby reducing equipment sizing. The raffinate off-gas of the PSA mainly consists of CO and hydrocarbons and serves as the feed gas for the reforming process. The PSAs modelled here follow a correlation developed by Nazir et al. based on four data points from high purity H_2 production in literature [19]. The correlation is expressed as follows, where P_1 and P_2 are PSA feed and off-gas stream pressures respectively:

$$H_2 recovery\ in\ PSA(\%) = 100 - \frac{100}{0.2521\left(\frac{P_1}{P_2}\right)+1.2706} \quad \text{- Eq\# 2}$$

A secondary PSA is similarly modelled at the tail end of the reforming process to separate out the makeup H_2 produced by reforming.

Gas compression is accomplished via a two-stage compressor train with intercooling. This keeps the temperature rise within a single compressor stage to within 500C while reducing compressor work.

The reformer pressure is lower than the ~33bar range found in the referenced literature [19]–[21], but it is well within the range of commercial reformers which typically operate from 15-40bar [37]. This pressure level was chosen to minimize the amount of gas compression required while at the same time having sufficient pressure to overcome the pressure drops

throughout the reforming process train in order to yield an output pressure at hydropyrolysis operating pressure.

Operating pressures in the model have four set points, from which MP steam pressure and all other pressure drops at every other point in the process are derived based on the pressure drop ratios defined in
. These set-points are:

- Incoming NCG pressure of 21bar
- PSA off-gas pressure of 1.1bar
- Hydropyrolysis reactor operating pressure of 22.4bar
- Reformer pressure of 25bar

In conventional natural gas steam reforming processes, the steam reacts with methane at high temperatures (>700°C) to generate H_2 and CO. The CO then further reacts with steam through the water-gas shift (WGS) reaction to form CO_2 and more H_2.

Hence in this modelled system, the pre-reformer functions to react C_{2+} gases and steam into CO and then methane, providing a methane rich product for the main reformer. It also reduces the propensity for coke formation in the main reformer. The pre-reformer reactions are also net exothermic thereby increasing the inlet temperature to the reformer and increasing the reformer's efficiency.

$$C_nH_m + nH_2O \rightleftharpoons nCO + (n + \frac{m}{2})H_2$$

$$CO + 3H_2 \rightleftharpoons CH_4 + H_2O, \qquad \Delta_R H = -206\frac{kJ}{mol}$$

The reformer is typically a fired tubular reformer (FTR) that requires an external furnace to provide the heat of reaction for the reforming process. Higher temperatures and higher steam to carbon (SC) molar ratios result in higher methane conversion to hydrogen. However, the process modelled here is constrained by the dual objectives to use only endogenously provided heat and water to produce steam and support the reaction. Hence the SC ratio was set at 2.7, within the range of commercially operated SMR plants[38] [39].

$$CH_4 + H_20 \rightleftharpoons 3H_2 + CO, \qquad \Delta_R H = 206\frac{kJ}{mol}$$

The modelled process also required both a high temperature and low temperature WGS reactor to produce sufficient hydrogen.

$$CO + H_2O \rightleftharpoons H_2 + CO_2, \qquad \Delta_R H = -41\frac{kJ}{mol}$$

To generate sufficient heat to support the reformer's endothermic heat requirements, generate steam for the reforming process and to produce electricity, two fuel sources are used: NCG off-gas from the PSAs, and char. For the former, the fraction is the maximum amount that will allow for the remainder to be reformed to produce sufficient makeup hydrogen. For the latter, the mass balance from the previous section gave the ultimate analysis of the char, but there was no proximate analysis information from the experimental data and hence it was not possible to characterise the char as a non-conventional solid in Aspen Plus. Hence for combustion, an equivalent amount of pure carbon with the same higher heating value (HHV) as the char from the mass balance was used. The HHV of pure carbon was obtained from literature at 32.77MJ/kg [40] while the HHV value of char from the mass balance was derived from equation 1. There could be better value-added uses for the char, either from an economic or carbon footprint basis, but this was not investigated in this study.

It should be noted that flue gas treatment was not modelled. Given the combustion of char which will contain much of the trace elements in the biomass feed, some form of gas treatment is likely necessary.

As for the steam system, the modelling did not investigate optimization of the steam network to maximize the efficiency of the power plant. Some optimization parameters that would need to be considered would be the steam property data, pressure levels for the heat recovery steam generator (HRSG), feed water heating, feed water flow path etc. The primary purpose of the NCG reforming modelling was to show that sufficient steam and hydrogen could be produced endogenously as well as to cover any internal electricity demands. The modelled system showed this to be the case, while any gains in net electricity output from a more optimized steam system would also be small compared to the energetic content of the biofuel product. Indeed the revenue from net electricity sales are also small compared to biofuel sales, all of which is further shown and discussed in Section 4.

Hence this study used the high pressure steam specification borrowed from other papers that modelled natural gas reforming [19]–[21]. The intermediate pressure steam level was determined by the reformer operating pressure. Low pressure steam was based on the lowest possible exit pressure from the LP turbine while maintaining a steam quality in excess of 90% given the turbine efficiency. Table 4 details the assumptions made for modelling the reforming process in Aspen Plus.

Table 4: Technical assumptions for NCG reforming process simulation in Aspen Plus

Process	Assumption
Thermodynamic properties	Peng-Robinson equation of state
Pre-reformer	• RGibbs reactor • Operating temperature: 600°C
Reformer	• RGibbs reactor • Steam:Carbon molar ratio = 2.7 • Operating conditions: 25 bar, 900°C
Water-gas shift	• REquil reactor • 350°C for high temperature reactor and 200°C for low temperature reactor
H_2 Pressure Swing Adsorber	• Separator block • 1% pressure drop on H_2 stream, off-gas pressure at 1.1 bar. • Separation based on correlation developed by Nazir et al. [19]
Heat exchangers	• MAT = 10°C for gas to liquid • MAT = 10°C for gas to steam • MAT = 20°C for gas to gas
Combustion chamber	• RGibbs reactor • Outlet temperature set at 1400°C to stay within material limitations • Flue gas to have minimum 5% molar fraction O_2 to ensure complete combustion
Combustion & ID fans	• $\eta_{isentropic}$=0.80, η_{drive}=0.97
Stack exit conditions	• ~110 °C and 1.05 bar
NCG Gas Compressors	• $\eta_{isentropic}$=0.87, η_{drive}=0.97 • Intercooling to 35 °C • Equal pressure ratio across stages
Cooling Water	• Source extraction at 15 °C, 1 atm, raised to 3 bar • Maximum ΔT=10 °C
Steam property data	• HP steam at 92 bar, 485 °C • IP steam at 26.6 bar, saturated – used for reforming • LP steam at 1.2 bar, 150°C
Steam Turbines	• $\eta_{isentropic}$=0.88, $\eta_{generator}$=0.97
Feed Water Pumps	• $\eta_{isentropic}$=0.80, η_{driver}=0.97
Pressure drops	• Reforming & WGS reactors: 1% of inlet pressure • Heat exchangers: 2% of inlet gas pressure

A sensitivity analysis on the Reformer operating pressure, temperature and steam to carbon ratio was also conducted. Details of results are elaborated in Section 4.1.2.

3.1.3. Auxiliary Systems

The auxiliary systems can be broken down into several subsystems:

- Biomass feed system
- Pyrolysis product separation
- Wastewater and gas treatment

Biomass feed system: IH2 has reportedly been tested on biomass feed particle size up to 5 mm [41], hence the wood feed would need to be sized before it can be fed into the process. It is assumed that the biomass arrives at site already appropriately sized within this specification and no further sizing is required on site, and hence there is not energy penalty for sizing of feed within the system boundary. However, a cost surcharge for feed sizing, and associated emissions is included in the calculations as detailed in the Section 3.3. In this study, the biomass feed handling system envisioned involves only a feed hopper with a rotary valve that feeds biomass into a direct contact steam belt dryer.

Thermal degradation of biomass becomes significant above ~120°C depending on the type of biomass which can lead to an increased risk of fire [42]. Using steam for drying has the advantage of providing an inert atmosphere which consequently allows for higher drying temperatures (up to 200°C) resulting in smaller equipment [43] [44]. To determine the heat requirements, this study assumes feed is dried from 30% to 5.6% moisture content to match the conditions of the experimental data, although in practice higher moisture levels going into the hydropyrolysis reactor can be accommodated. Low pressure superheated steam data for this service is assumed to be 1.2bar and 150C. This is the same pressure level as the low-pressure steam in the NCG reforming process, but in this study the steam flows for feed drying are considered separate from the steam system in the reforming process since the steam flows required for feed drying are considerably higher than in the reforming process. There is likely scope for integration of the two systems for greater efficiency gains, but this was not investigated in this study.

Drying the biomass involves heating the biomass from 25-104°C, which is the saturation temperature of the drying steam and the temperature at which the biomass is assumed to enter the hydropyrolysis reactor, plus the heat to evaporate the moisture in the feed. This results in a drying load of 930kW/$kg_{biomass\ a.f..}$. It is assumed that the drying system has an efficiency of 80% which in turn means that a heating load of 1163 kW/ $kg_{biomass\ a.f.}$ is required. This heat is assumed to be supplied via the heat of pyrolysis since the hydropyrolysis and hydroconversion processes are exothermic. This is described further in the pyrolysis product separation system description below.

Large amounts of steam are required since the available superheat from 150-104 °C is small per unit steam flow rate. The steam flow rate is calculated at 12.73 $kg_{LPsteam}/kg_{biomass\ a.f.}$ Hence for start-up an alternative source of heat energy will be required although this consideration is neglected in this study. The drying process will evaporate moisture from the feed in the form of saturated steam, adding to the mass flow of the drying steam. This evaporated moisture is then bled off from the main drying steam flow. In this study it is assumed this heat is wasted although it can almost certainly be used for various plant needs.

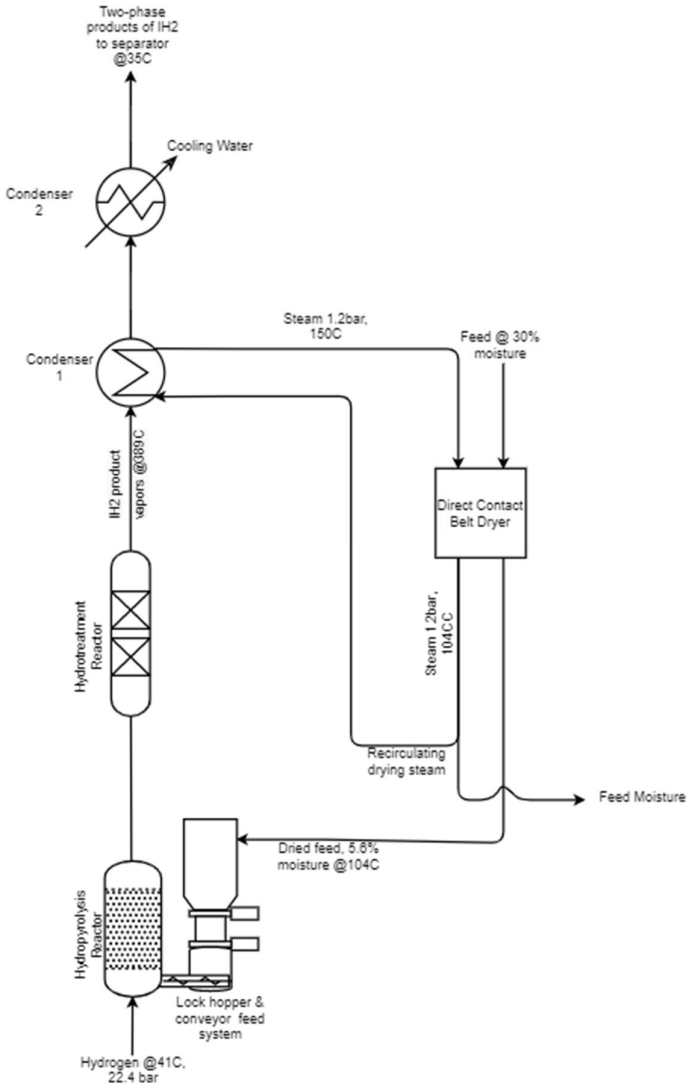

Figure 5: IH2 biomass drying and feed system

After the belt dryer the feed then goes into a buffer hopper and then into a pressurized feed screw conveyor which the enters the reactor. The buffer hopper and screw conveyor are separated by a lock hopper with isolating gate vales on either side. The pressurized environment is provided by hydrogen since it is used by the hydropyrolysis process anyway. The lock hopper system is a proven system that avoids common material handling issues into a pressurized environment such as clogging, excessive wear and tear, pressure sealing issues and spontaneous ignition [45]. Power requirements for the feed system described above is assumed at a rate of 5.6kWh/$T_{biomass\ a.r.}$ for the handling system of conveyors and 2.0kWh/$T_{biomass\ a.f.}$ for the lock hopper system [18], resulting in a total electrical load of 34.4kJ/ $kg_{biomass\ a.f.}$.

Pyrolysis product separation: Downstream of the hydroconversion process, the product stream is cooled resulting in the condensation of water vapor and the liquid HC product which are then separated out. The composition of the liquid HC product is unknown and hence the thermodynamic data necessary to calculate an overall value for the heat of condensation of the pyrolysis vapours had to be estimated. This is an important energy source and is one of the major advantages of the IH2 process. In this study, this heat was envisioned to be used

for feed drying purposes as described above under the biomass feed system, completely separate from the steam system in the NCG reforming process. Osborne and Ginnings [46] measured the heat of vaporization and heat capacities of a number of hydrocarbons. The results showed these values to be within a narrow range for all the hydrocarbons tested. Indeed, this was confirmed by trial modelling the condensation of various longer chain HC vapours with the other known products of hydrpyrolysis in Aspen Plus from the hydroconversion exit temperature of 389°C to 115°C (~LP steam saturation temperature + MAT). Then a conservative value obtained from Aspen Plus for the condensing heat from among the measured hydrocarbons by Osborne and Ginnings [46], and including the other known vapours as reported in the experimental data was used. This value was 1300 kW/$kg_{biomass\ a.f.}$ which is well above the 1163 kW/ $kg_{biomass\ a.f.}$ required for feed drying. Hence it was assumed the difference were losses in heat transfer to low pressure steam resulting in a heat exchanger efficiency of ~90%.

Wastewater and gas treatment: The wastewater system functions are required to clean the water condensed out of the vapor stream from the two reactors. The water at this point contains various contaminants such as ammonia and sulphates that must be removed. The technology developer envisions a sour water stripper that removes the ammonia and dissolved hydrogen sulphide before further treatment. The treatment could be even more complicated than this should the water be recycled to become boiler feedwater. The stripped ammonia and hydrogen sulphide join the NCGs at a scrubber just upstream of the reformer where any contaminants are also stripped from the NCGs. The ammonia and hydrogen sulphide can then be turned into saleable aqueous ammonia and ammonium sulphate. Neither the wastewater treatment nor gas treatment systems are modelled here. The electrical demands are assumed to be minimal, although costs are included in operational cost calculations as described in Section 3.3.2.

3.1.4. Liquid Product Refinement

A detailed chemical breakdown of the liquid fuel product from the IH2 process is not presented by the technology developer in their published literature, as can be seen from Table 4. However various specifications for cut points which they deem to be gasoline and diesel blend stocks are presented. This data can then be compared against a suitable fuel standard to determine reasonable assumptions for additional processing at a downstream refinery. This data is shown in Table 5 and Table 6 where it is compared against the Worldwide Fuel Charter Category 4 gasoline and diesel specifications respectively. This category comprises advanced emissions control requirements such as Euro 5 and 6 fuels, and hence reflects the current best in class standards in Europe [47]. The comparison table does not display all the Category 4 specification of gasoline and diesel, only those for which IH2 experimental data from woody biomass fuel was published.

Table 5: IH2 gasoline Product Characteristics from mixed wood feed comparison with category 4 fuel standard

Gasoline Product Comparison		
	IH2 [9], [10]	Category 4 [48]
Oxygen, %wt	1.0	2.7 (max)
Sulphur, ppm wt	52	10 (max)
Density @15°C, kg/m^3	0.761-0.790	0.750-0.770
Final boiling point, (°C)	220	205
T90 distillation point, (°C)	173	130-175
RON	87	95 (min)
Aromatics, %vol	37	35 (max)
Olefins, %vol	<1	10 (max)
Benzene, %vol	0.87	1 (max)

Table 6: IH2 diesel Product Characteristics from mixed wood feed comparison with category 4 fuel standard

Diesel Product Comparison		
	IH2 [9], [10]	Category 4 [48]
Sulphur, ppm wt	52	10 (max)
Density @15°C, kg/m^3	0.936-0.952	0.815-0.840
Viscosity @40°C, cst	7.6	2.0-4.0
Flash Point	156	55 (min)
T90 distillation point, (°C)	341	320 (max)
Cetane Index	22	52 (min)
Aromatics, %wt	83	15 (max)

The technology developer asserts that the gasoline produced from woody biomass feedstock would only require blending at the refinery. Indeed, the data seems to bear this out. For the diesel product, however, the aromatics content is far too high resulting in a low cetane number. Other characteristics such as density, viscosity and sulphur content are also too high. This indicates that the diesel product will require further hydroprocessing for aromatic saturation, sulphur removal and cracking of larger HC chains at a refinery to bring the product within specification [9].

The above conclusions were also reached by Jafri et al. [49] and Furusjö et.al [6] whereby it was assumed that gasoline goes straight to blending without further processing whereas the diesel product would require an additional 0.17 MW/MW$_{biofuel}$ of H_2 at the refinery via a Synsat process based on stoichiometry. It was further assumed that the weakly endothermic Synsat process would require no additional external heat. At this rate, hydrogen required at the refinery is just under 5%wt of the biofuel which aligns with the range reported in literature [25]–[28]. Hence this study makes the same assumptions for the refinery, while also assuming that all the hydrogen is absorbed into the refined diesel product for mass and energy balance purposes.

3.2. Process Performance Evaluation

The IH2 process modelled as per the preceding subsections was then evaluated for technical performance using different measures of efficiency within the system boundary. Energy parameters were on HHV basis. Several metrics were used for this purpose:

- Carbon recovery in HC liquid product

$$Carbon\ Recovery = \frac{Mass\ of\ Carbon\ in\ HC\ Liquid\ Product}{Mass\ of\ Carbon\ in\ Feed}$$

- HC liquid product yield

$$Yield_{HC\ Liquid\ Product} = \frac{Mass\ of\ HC\ Liquid\ Product}{Mass\ of\ Feed\ d.a.f.}$$

- Conversion Efficiency

$$\eta_{conversion} = \frac{HC\ Liquid\ Product\ Energy}{Feedstock\ Energy}$$

- System Efficiency

$$\eta_{system} = \frac{Output\ Energy}{Input\ Energy}$$

System efficiency expands on conversion efficiency by including other exogenous energy inputs required for biofuel production such as natural gas, hydrogen or electricity. In the IH2 process, there is an electricity surplus generated endogenously while external hydrogen supply is required at the refinery. For the other three process routes, primary energy inputs will variously require additional inputs of biomass (for hydrogen production from biomass gasification), electricity (for hydrogen production from electrolysis) and natural gas (for hydrogen production from reforming) in addition to hydrogen at the refinery.

HHV was used for energy calculations for the technical evaluation of the process. The values were either obtained from literature [50], or in the case of biomass feed, char and gasoline product, calculated using equation #1.

LHV was used in economic and GHG emissions calculations due to values from ENPAC being on an LHV basis (refer to section 3.3 below). LHV was obtained in two ways. For the refined diesel product, since the ultimate analysis is not known after treatment through the refinery, a value of 43 MJ/kg was used from literature [50]. For biomass and gasoline where the HHV was calculated using equation #1, LHV was calculated using the formula below.

$$LHV = HHV - M(9H + E)\ \text{MJ/kg} \text{ - } \mathbf{Eq\#\ 3}$$

where *E* is the heat of evaporation of water (2.441 MJ/kg), while *H* and *M* are the weight proportion of hydrogen and moisture contents of the energy carrier respectively [51]. Appendix B summarizes the various HHV and LHV values used in this study.

3.3. Economic and GHG Assessment

The method by which the IH2 process' viability was assessed with respect to economic performance and emissions impact is described below. The methodology aims to develop meaningful measures to evaluate the technology but at the same time provide the framework for comparison with the other three process routes in the larger project using these very same metrics.

3.3.1. ENPAC

In this study, the pricing of process inputs and outputs such as biomass feed, bio-oil output electricity deficit/surpluses and GHG emissions was achieved using the Energy Price and Carbon Balance Scenarios (ENPAC) tool. The tool was developed at Chalmers University to aid in assessing the long-term viability of industrial energy projects [52]–[54]. The tool calculates future energy prices for large-volume energy users located in Northern Europe. A graphic overview of the tool is shown in Figure 6.

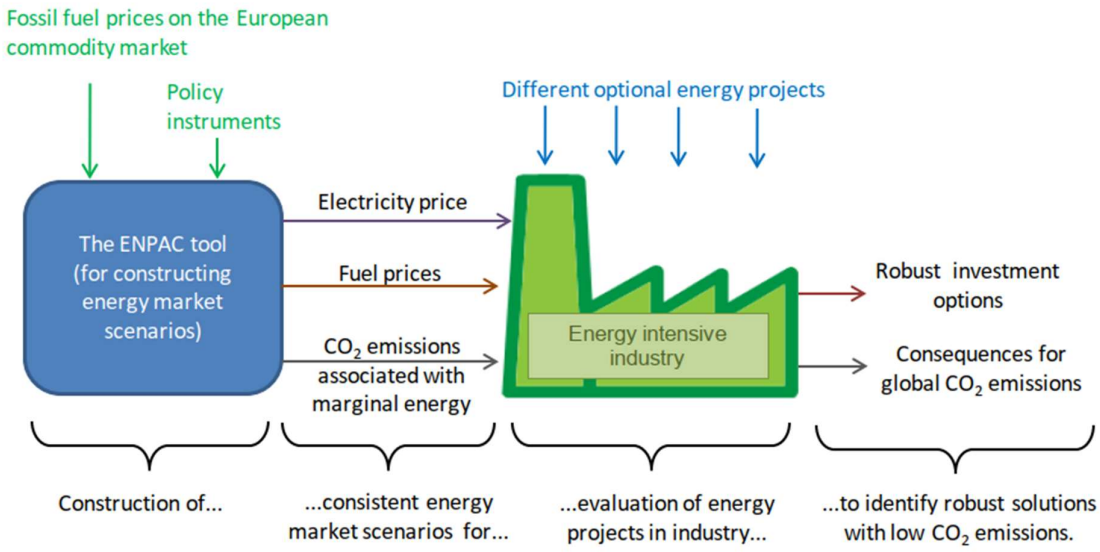

Figure 6: ENPAC tool energy pricing overview

Comparing the viability of alternative energy projects is subject to significant uncertainty. The way ENPAC can be used to deal with this uncertainty is by generating consistent sets of user-defined future energy market scenarios. The standard way to use the tool is by using input data for fossil fuel prices from the scenarios published in the IEA's World Energy Outlook (WEO) [55]. The data used in this report was WEO 2017. The assumptions within each of the scenarios are then used to calculate future energy carrier prices, and indicative values of GHG emissions associated with those carriers. These prices are not a forecast into the future, but rather a set of consistent energy market parameters given certain scenario conditions. The three scenarios included in WEO 2017 are:

- The Current Policies Scenario (CP) – represents the current situation without any changes in policy
- The New Policies Scenario (NP) – Incorporates already announced policies and targets
- The Sustainable Development Scenario (SD) – a back casted calculation on fossil fuel prices, policy and support levels that would be required to reach net-zero GHG emissions aligned with the Paris Agreement

The user inputs to ENPAC are raw fuel prices (e.g. Brent crude, thermal coal and natural gas prices) for regional markets, CO_2 emission charge similar to the EU ETS emissions permit price, and various assumptions such as which marginal electricity technologies should be available, price support for renewable energy or biofuels and whether biomass is to be considered a limited resource. ENPAC then calculates future prices for large-volume industrial consumer for various energy carriers based on consistent energy conversion technology characteristics and substitution formulas.

The following ENPAC output categories are used in this study:

- **Gasoline & Diesel price:** Based on a historical correlation formula between the Brent crude oil price and gasoline/diesel product prices including any GHG emissions charges on the fuel.
- **Biofuel price:** Based on the concept of "Willingness to Pay" (WTP). This concept assumes that the consumer is only willing to pay the same amount for a biofuel as they would for the equivalent fossil fuel at the pump. Hence the selling price of the biofuel for the producer (i.e. 'gate price') is equal to the price of the equivalent fossil fuel at the pump, including any GHG emissions charges on the fossil fuel, minus

any distribution and GHG emissions charges associated with the biofuel, plus any subsidy support. In this study, Fischer-Tropsch Diesel and Gasoline (FTD & FTG) prices from ENPAC are used as proxies for the gasoline and diesel biofuels produced by the IH2 process.

- **Biomass price:** The price of low-grade biomass is based on the marginal user of biomass with the highest WTP. The two price setting marginal users considered in ENPAC are production of pellets for co-combustion in a coal-fired condensing power plant or wood chips used as feedstock for a biofuel production plant. Hence, for the former, the WTP for pellets is directly related to the price of thermal coal including the associated CO_2 emissions charge, pellet production costs and renewable energy support levels while for the latter, the WTP for biomass depends on the price of liquid fossil fuels including CO_2 emissions charge, biofuel production costs and level of biofuel support.
- **Electricity wholesale price**: Based on the power generation technology with the lowest levelized cost of electricity generation (LCOE) inclusive of capital investment costs in the base-load market. This 'build-margin' technology sets the emissions and costs for the marginal user of grid electricity. ENPAC considers Wind, Nuclear, Coal, and Natural Gas Combined Cycle (NGCC) as potential build-margin technologies with the latter two considered with and without CCS. The price of sold and purchased electricity are different due to the additional transmission cost associated with the latter. For wind, the selling price is based on the wholesale market price with a green electricity premium added.
- **GHG emissions factors:** Emissions factors are applied to various fuels and electricity production based on plant and combustion efficiencies and emissions from combustion.

Full details of how ENPAC calculates various price and emissions values are found elsewhere [52]–[54]. The ENPAC version used in this study was '*version 2.1x, 2019-11-13*'.

This study uses the ENPAC outputs for the NP and SD scenarios in 2030 for the economic analysis. The CP scenario does not add much value to the analysis since the outputs do not differ significantly to the NP scenario while also representing an unlikely worst-case scenario. It is reasonable to expect that currently announced policies will at least in part be enacted in the coming years, if not strengthened. The SD scenario on the other hand represents the other bookend on what is possible and is hence used in this study to represent an ideal case. 2030 is chosen as the future comparison year as it represents a reasonable time frame by which time the technology pathways have a viable chance of being in commercial operation.

The main difference between the NP and SD scenarios is the CO_2 emissions charge applied to fossil fuels. In the SD scenario, the CO_2 charge is higher resulting in lower base liquid fossil fuel prices (i.e. excluding the CO_2 charge) due to reduction in demand. Further, in the SD scenario biomass is considered a limited resource. This means that any marginal user of biomass, such as the IH2 plant considered in this study, would effectively be procuring feedstock otherwise used by the previous marginal user with the highest WTP as described above. It also means that the cost of biomass is higher than in the NP scenario due to its scarcity. In the NP scenario where by 2030, biomass is still not a limited resource, the emissions are only related to harvesting, transport and pre-treatment of the biomass feedstock. This assumption is judged reasonable for the NP scenario given the current forecasts of biomass surplus in Sweden for bioenergy usage [3].

This study also assumes the level of support for biofuels and CO_2 emissions charges are equivalent to the current levels in Sweden in keeping with the objective of the study to be

grounded in the Swedish context, as opposed to the pan-European averages forecasted in IEA's WEO 2017 scenarios.

The pricing of hydrogen is calculated as 3.564 times the price of natural gas produced via SMR, on a mass basis. The multiple represents the average of a low and a high estimate [6], [38], [56] in the literature. Hydrogen pricing is required to determine the cost of refining IH2 diesel at the refinery as explained in Section 3.1.4. Emissions from hydrogen production via SMR is estimated as 91.4 g_{co2eq}/MJ_{LHV} [6], [38], [56]. The emissions charge is applied on well-to-wheel emissions for the energy carrier applying only to CO_2, while a CO_{2eq} basis is for calculation of GHG emission balances.

The ENPAC inputs and outputs used in this study are shown in Table 7, with currency values corresponding to base year 2019 for the 2030 SD and NP scenarios. The choice of 2019 was taken over 2020 to avoid the distorting impact of the COVID epidemic on the world economy. Further all per MWh units displayed below are on an LHV basis for non-electricity energy carriers. This contrasts with the technical evaluation which was done entirely on an HHV basis.

Table 7: ENPAC economic inputs and outputs used in this study

ENPAC inputs	Units	Scenario	
		2030-SD	2030-NP
Fossil Fuel Inputs			
Crude Oil (Brent)	$/Barrel	69	94
	€/MWh	39	52
Natural gas EU import price	€/MWh	25	29
Biomass availability			
Biomass as a limited resource		Yes	No
Policy instruments & taxes			
EU ETS CO2 charge	€/ton	79	29
Support for renewable electricity	€/MWh-el	5	5
CO2 charge for gasoline	€/ton	99	99
CO2 charge for diesel	€/ton	110	110
Support for diesel biofuels	€/MWh-fuel	25	25
Support for gasoline biofuels	€/MWh-fuel	43	43
Outputs			
Electricity build margin technology		Wind	Wind
Electricity (seller)	€/MWh-el	45	45
Electricity (buyer)	€/MWh-el	48	48
Natural gas (buyer), w/CO2 charge	€/MWh-fuel	48	41
Hydrogen	€/MWh	67	57
Marginal user of wood fuel		Pellets	FT
Wood fuel (buyer)	€/MWh-fuel	27	16
Biofuel (gasoline) - sale price at gate, incl. support	€/MWh-fuel	114	128
Biofuel (gasoline) - sale price at gate, excl. support	€/MWh-fuel	71	85
Biofuel (diesel) - sale price at gate, incl. support	€/MWh-fuel	106	122
Biofuel (diesel) - sale price at gate, excl. support	€/MWh-fuel	81	97

3.3.2. Economic Evaluation

In this study the economic viability of the IH2 process was calculated from the operating costs (OPEX) per unit of produced biofuel energy (in $€_{2019}/GJ_{LHV\text{-}biofuel}$) and then comparing it to the potential revenue of the plant from selling biofuel. This would also give an indication on the capital investment that can be supported.

This study did not attempt to independently establish a Total Capital Invested (TCI) estimate to construct a new IH2 facility. TCI estimates for a IH2 plant have previously been attempted by the technology developer and Meerman & Larson which then formed the basis of their respective techno-economic analyses [11], [18]. The CAPEX estimates in both studies are built up by sizing the major equipment from process modelling and then costing this equipment by applying an equipment sizing scaling factor to reference costs for similar components from published sources, or supplier quotations and consultations. On top of this cost, percentages are added for balance of plant, indirect costs and contingencies to estimate the TCI. This factored estimation methodology results in a scoping level estimate for a novel technology.

Hence the estimates need to be considered critically. Further, both estimates feature some differences in their respective plant configurations. For example, Meerman & Larson's plant featured a turbine for electricity generation whereas the technology developer's plant produced heat instead. It was also considerably larger thereby benefiting from economies of scale when using factored estimation of costs. This renders direct comparison between the two estimates more complicated.

The Aspen Plus model in this study could have been used to provide some capital cost estimates based on the modelled equipment sizing. However, any estimates derived from the Aspen model would have excluded the main hydropyrolysis and hydroconversion reactors and many of the auxiliary systems that were not modelled rendering any potential TCI estimates incomplete. Further, there is likely very little value in developing a new TCI estimate for an IH2 plant given firstly, how difficult this is to do for novel technology, and secondly, not providing any additional insights beyond the two already published estimates without more recent and detailed plant operating data that is only available to the technology developer.

The TCI estimates are reproduced here in Table 8 and are used in this study for reference to evaluate the viability of a proposed plant based on the operating expenditures versus biofuel selling price. The estimate by Meerman & Larson has been modified to an n^{th}-of-a-kind (NOAK) plant estimate by removing the factor of 2 that was applied for a first-of-a-kind (FOAK) plant to provide a comparison to the technology developer's NOAK estimate. The differences in the specific TCI can be attributed to different plant configurations, different contingencies and the effect of scale given Meerman & Larson's considerably larger plant size.

Table 8: IH2 CAPEX estimates from published literature

	Units	Tan et al. [19]	Meerman & Larson [24]
Biofuel Production	MW_{HHV}	260	493
	MW_{LHV}	244	463
Feed rate	T_{dry}/day	2000	3425
TCI	$MUS\$_{2007\ \&\ 2014}$	264	306
	$M€_{2019}$	223	243
Specific TCI	$M€_{2019}/MW_{biofuel\ LHV}$	0.91	0.53

Operating expenditures were built up using input from the process model, ENPAC and costs from the technology developer's operating cost estimate for a 2000 $T_{d.b}$/day plant [11]. Various important assumptions, beyond those described in Sections 3.1 and 3.3.1, were made to build-up this estimate. Feed was considered to come to the plant appropriately sized. Hence a surcharge for sizing was added to the ENPAC derived cost for biomass feed. This surcharge was calculated based on an electrical load requirement of 0.05 $kWh/kg_{biomass\ a.r.}$to run a hammermill to size the coarse biomass feed to under 5 mm [57]. Maintenance costs are assumed to be 5% of the average of both annualized specific TCI estimates in Table 8. Revenue from ammonia and ammonium sulphate is disregarded for two reasons. Firstly, the quality of these products produced by the plant is not revealed by the technology developer and hence it is difficult to estimate an appropriate sales price. Secondly, revenues from these by-products only represent a small percentage (<1.5%) of the technology developer's operating expenditure estimate [11].

All prices and estimates used in this study are in 2019 Euros, as described in Section 3.3.1. The Chemical Engineering Plant Cost Index (CEPCI) was the principle tool used to escalate costs into 2019 currency [58]. Labour costs used the construction labour CEPCI data subset

whereas other plant costs used the composite CEPCI index values. Currency conversions were done using the Swedish Riksbanken annual average exchange rate [59].

$$Non\ labor\ OPEX_{2019} = \frac{CEPCI_{composite\ yr-i}}{CEPCI_{composite\ 2019}} * 2019\ €:\$\ annual\ avg\ exchange\ rate \text{ - Eq\# 4}$$

$$Labor\ OPEX_{2019} = \frac{CEPCI_{constr\ labor\ yr-i}}{CEPCI_{consr\ labor\ 2019}} * 2019\ €:\$\ annual\ avg\ exchange\ rate \text{ - Eq\# 5}$$

The difference between the selling price of gasoline and diesel, as obtained via ENPAC, and the calculated OPEX would indicate the TCI that a prospective producer can afford while remaining profitable. To calculate what this value could be, the following is assumed as per Table 9.

Table 9: Assumed values for maximum supportable TCI

Plant availability	96%
Interest rate	8%
Plant life (yrs)	20
Annuity factor	0.10
Minimum specific operating margin	15%

Further, the specific operating margin, expressed in terms of €/$GJ_{LHV\ biofuel}$, is defined as:

$$Specific\ Operating\ Margin = \frac{Biofuel\ avg.sales\ price - Spec.OPEX - Spec.TCI}{Biofuel\ avg.sales\ price} - Eq\#6$$

Then assigning the minimum specific operating margin of 15% to Equation 6, the specific TCI can be solved for.

It should be noted that the nominal feed rate of 1 kg/s of biomass a.f. used in this study was chosen to express mass and energy balance results on a per unit feed a.f. basis for convenience, which can then be scaled up depending on plant size. However, there would be technical efficiency gains with scale that would not be evident when scaling linearly. Similarly, when conducting an economic assessment, cost scaling for different plant sizes can only be done reasonably within limited size ranges, since below a certain size unit costs become very large while above a certain threshold plant sizes are no longer practical. Hence the plant sizes in Table 8 could be seen as probable ranges (i.e. ~25kg/s to 42 $kg/s_{biomass\ a.f.}$) for which an actual commercial scale plant would feasibly be built. Hence when the various cost parameters in this study in Section 4.2 are expressed in terms of €/$GJ_{LHV\ biofuel}$, the values have to be understood within this context, i.e. that the values cannot be scaled indiscriminately for a wide range of plant sizes and that some engineering judgement must be used.

3.3.3. GHG Emissions Evaluation

Similar to the economic evaluation, the GHG emissions were evaluated on a per unit GJ of biofuels on an LHV basis. However, emissions are now inclusive of other GHG emissions other than CO_2 and hence the numerator is expressed in kg_{CO2eq}. The emissions values used are from ENPAC and are shown in Table 10

Table 10: ENPAC GHG emissions for various energy carriers

Emissions (kg_{CO2eq}/MWh)		
Energy Carrier	SD	NP
Electricity from grid	0	0
Biomass usage	405	8
Hydrogen	329	
Gasoline well-to-wheel	286	
Diesel well-to-wheel	289	

ENPAC emissions values for biomass do not include any direct or indirect land use change effects since the feedstock is considered forestry residues. Hence, the footprint associated with the feedstock is only related to collection, transportation, and processing. Additional GHG emissions related to feed sizing are due to electricity usage. However as discussed in the previous section, the build margin for both scenarios in 2030 is Wind power resulting in zero emissions attributed to electricity usage or supply. On the other hand, the IH2 process is a net electricity supplier and hence does not get credit under these scenarios either.

The SD scenario has an especially high emissions value associated with biomass. This is related to the fact that in the SD scenario, biomass is considered a limited resource and the marginal user is assumed to be a coal fired power plant that uses biomass in the form of pellets for co-firing. The combination of these two assumptions means that any competing user of biomass, in this case the IH2 process, would indirectly force the marginal coal power plant to procure more thermal coal to make up for the biomass shortfall resulting in increasing emissions overall.

Emissions from hydrogen production via SMR is estimated as 91.4 g_{co2eq}/MJ_{LHV} [6], [38], [56].This value is used to attribute emissions to the refining of the IH2 diesel product where an exogenous source of hydrogen is required. Although the emissions impact of hydrogen usage at the refinery is included, the emissions from transportation of the biofuel from the IH2 facility to the refinery, and then again to the consumer is disregarded as it is assumed to be small. For reference the technology developer estimates IH2 product transportation emissions to be on the order of 1.25 $kg_{CO2eq}/GJ_{LHV\ biofuel}$ while Zupko estimates this value at 0.6-0.7 $kg_{CO2eq}/GJ_{LHV\ biofuel}$ [12], [22].

The emissions balance comparison that is done between the IH2 biofuels and fossil fuel equivalents are expressed on a well-to-wheel basis and hence expand upon the system boundary as show in in Figure 3. Biogenic emissions are considered as net zero in ENPAC, hence any emissions from the stack of the IH2 process are disregarded.

4. Results & Discussion

4.1. IH2 Process Modelling

The section below details the results from the black box mass balance of the IH2 reaction process, the NCG reforming Aspen Plus model with process parameter sensitivity analysis, the overall system boundary energy and mass balance and finally the process performance.

4.1.1. Hydropyrolysis & hydrotreatment black box mass balance results

The results of the IH2 process modelling are presented in this section. Table 10 shows the breakdown of the input biomass to the hydropyrolysis reactor after drying at a nominal feed rate of 1 kg/s:

Table 11: IH2 input mass balance

Hydropyrolysis reactor input (kg/s) - a.f. basis							
Input:	C	H	O	N	S	Ash	Total
Biomass	0.469	0.055	0.414	1.04E-03	2.83E-04	0.005	0.944
Moisture	-	0.006	0.050	-	-	-	0.056
Total	0.469	0.061	0.464	1.04E-03	2.83E-04	0.005	1.000

Table 12: IH2 output mass balance

Elemental breakdown of products (kg/s) - a.f. basis								
Output:	C	H	O	N	S	Ash	Total	wt%, DAF
CO	0.026	-	0.035	-	-	-	0.061	6.50%
CO2	0.019	-	0.051	-	-	-	0.070	7.40%
CH4	0.026	0.009	-	-	-	-	0.035	3.73%
C2H6	0.050	0.013	-	-	-	-	0.063	6.68%
C3H8	0.031	0.007	-	-	-	-	0.038	4.09%
C2H4	-	-	-	-	-	-	0.000	0.00%
C3H6	-	-	-	-	-	-	0.000	0.00%
Char	0.104	0.002	0.019	1.37E-04	2.36E-04	0.005	0.131	13.40%
Water	0.001	0.045	0.357	8.23E-04	3.48E-05	-	0.404	37.00%
Liquid	0.211	0.028	0.002	7.81E-05	1.26E-05	-	0.242	25.80%
H2 reactant	-	-0.043	-	-	-	-	-0.043	-4.60%
Total	0.469	0.061	0.464	1.04E-03	2.83E-04	0.005	1.000	

Table 12 shows the output from the hydrotreatment reactor. Any elements that did not balance as per the adjusted experimental results in Table 2 had the balance assigned to char. From here the ultimate analysis of the liquid HC product was determined using a combination of Table 2 and Table 3 shown in Table 13

Table 13: Liquid HC product ultimate analysis

IH2 Liquid Hydrocarbon Product Characteristics, w/o Refinery, from Mass Balance							
HC product:	C	H	O	N	S	HC Ratio	HHV (MJ/kg)
Gasoline	0.139	0.020	0.002	2.59E-05	8.32E-06	1.7	44.70
Diesel	0.073	0.008	0.001	5.22E-05	4.28E-06	1.3	42.50

The heating value is calculated using equation 1. The HC ratio matches the experimental data while the percent error from the mass balance of the liquid product in is within 2% of experimental data. Table 12 lists the NCG mass flows that were then fed into the NCG reforming Aspen Plus model to determine if the system could generate sufficient replacement hydrogen of 0.043 kg/s, while at the same time providing enough energy and steam for the reforming process.

4.1.2. NCG reforming Aspen Plus model results:

Gas Conversion: The stream data for each point in the process is shown in Appendix C. In the system as modelled, 0.027 $kg_{H2}/kg_{biomass\ a.f.}$ enters the reforming process after the Primary PSA. After reforming and WGS, and before the secondary PSA, the system has produced 0.056 $kg_{H2}/kg_{biomass\ a.f.}$ This value is in surplus over the required makeup hydrogen rate of

0.043 kg/s, but the surplus is required to have sufficient hydrogen exiting the secondary PSA which operates according to the correlation in Equation 2. The off-gas raffinate from the secondary PSA and a bleed of ~4.8 wt% of the raffinate off-gas from the Primary PSA goes to the combustion furnace, which along with the char provides all the energetic requirements of the process. The gas total to the furnace is 3.31 $MJ_{NCG\text{-}to\text{-}furnace}/kg_{biomass\ a.f.}$, which is comparable calorifically to the 3.71 $MJ_{char\text{-}to\text{-}furnace}/kg_{biomass\ a.f.}$ co-combusted with the NCGs in the furnace for heat. The reactions in the pre-reformer show the conversion of C_2H_6 and C_3H_8 to CH_4 as expected, while the reformer does most of the heavy lifting for hydrogen production with the two WGS reactors adding to this amount to a smaller extent. Hence it can be seen that the IH2 process can produce sufficient hydrogen endogenously to produce a HC liquid product. This gas species conversion progression is shown in Figure 7.

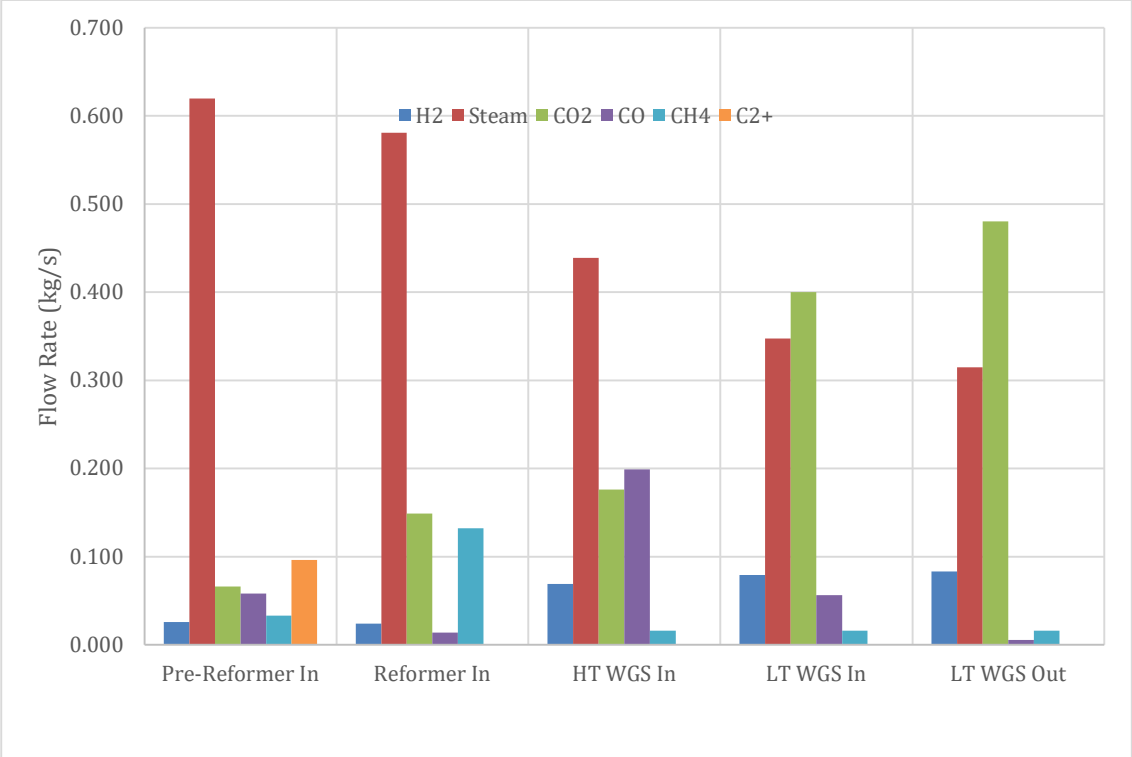

Figure 7: Reforming process gas species conversion progression

Electricity balance: The electricity balance of the plant is shown in

Table 14 14. The steam produced by the combustion furnace and heat recovery from various sections of the process were assumed to be used to produce steam which was in turn used for reformation and to produce electricity. The electricity was generated by a high pressure and low-pressure turbine. The exit pressure from the HP turbine was the same pressure as steam reforming pressure, and hence this steam was partially bled for the main process. The remainder was fed to the low-pressure turbine. Internal loads within the reformer process are compressors, blowers and boiler feedwater pumps. Loads from the rest of the plant are the feed handling system and 'other plant loads', estimated at 15% of the listed internal loads meant to represent balance of plant related loads. Hence even without optimization of the steam system the reformer model produces roughly double the electricity required to power internal consumption, with the remainder sold to grid.

Table 14: IH2 Plant overall electricity Balance

Electricity Consumer	kW

HP Turbine	419
LP Turbine	508
Comb blower	-36
ID Fan	-52
FW Pumps	-21
Compressors	-266
Feed handling	-34
Other plant loads	-61
Net ($k/kg_{biomass\ a.f.}$)	457

Sensitivity: As detailed in Section 2, the reforming process flowsheet was not optimized to this specific composition of feed gas species, rather it was adapted from SMR models published in literature. The reforming process has three process variables that are key to its conversion efficiency: pressure, temperature, and SC ratio. This section investigates the sensitivity of the model to changes in these process variables.

SC ratios are typically significantly higher than stoichiometric resulting in the excess steam having to be heated up to reformer temperature and then cooled down again post reformer resulting in lower efficiency. Higher SC ratios also result in increasing equipment size and hence cost. However, this excess prevents the formation of solid carbon compounds that can plug up catalyst and allows for more complete consumption of HC gases to produce more H_2. Higher temperatures play the same role; hence some combination of higher SC ratios and higher temperatures is typically selected for reformer operations. Higher pressures on the other hand result in less methane conversion and consequently lower hydrogen production. But higher pressures are employed for various practical reasons. For example, higher pressures result in smaller equipment sizes for the same gas flow rates. Further the PSA requires higher pressures to operate efficiently and it is cheaper to compress boiler feedwater and the NCGs prior to reformation than after reformation when water is in the form of steam [60]–[62]. SC ratios are typically 2.7-4.5, with reformer temperatures and pressures from 800-900 °C and 15-30 bar, respectively[21]. With this theoretical understanding, the process sensitivity to these three process variables can now be examined as per the tables below, with green highlights indicating the base modelled case.

For the SC ratio, the Aspen Plus model is set up such that the amount of gas bled from the NCG stream exiting from the primary PSA to the combustion furnace is as high as possible, while allowing the main NCG stream to produce the required amount of makeup hydrogen consumed by the IH2 process. Since higher SC ratios require less NCGs to produce the required makeup hydrogen, it follows that a greater proportion of the NCG stream will also be bled from the primary PSA. However as explained above, higher SC ratios have a negative effect on efficiency and result in increased equipment sizing, on top of more steam bleed from the turbine resulting in less electricity production. Hence the SC ratio would ideally be as low as possible to prevent formation of carbon species deposits on the catalyst, the level of which is not revealed in the Aspen Plus simulation as currently modelled, while still producing sufficient makeup hydrogen. The amount of methane remaining unconverted at the exit of the LT-WGS reactor and electricity generated is lower with higher SC ratios as expected. All the SC ratios examined produced excess H_2 indicating that there are efficiency gains to be made by lowering the SC ratio further with the caveats mentioned above. Table 15 shows these results, it should be noted only the net amount of electricity generated by the turbine minus power consumed by the compressors and blowers is shown.

Table 15: SC ratio sensitivity
Values in green are base modelled case

SC Ratio	Excess H_2 (g/s)	CH_4 ex. LT-WGS (g/s)	Net Electricity (kW)
2.40	13.18	21.32	615
2.70	13.96	16.20	588
2.94	14.41	13.22	567
3.21	14.80	10.63	542
3.49	15.08	8.70	512

Varying temperature from 850-925°C shows a similar trend to increasing the SC ratio as expected. The model is able to produce sufficient hydrogen even at 850 °C indicating that it is possible to operate at even lower temperatures. Indeed, literature sources indicate that at a high SC ratio (~3), methane can be completely consumed without a risk of formation of solid carbon species above 720 °C, although reformers typically operate above 800 °C [60].

Table 16: Reformer temperature sensitivity
Values in green are base modelled case

Reformer Temperature (°C)	Excess H_2 (g/s)	CH_4 ex. LT-WGS (g/s)	Net Electricity (kW)
850	11.96	34.72	687
875	12.64	25.75	619
900	13.96	16.20	588
925	14.81	10.19	584

When varying reformer operating pressure from 25 to 40 bar, less hydrogen is produced in the reformation process which is partially balanced by the higher efficiency of the secondary PSA since a higher pressure differential results in better hydrogen selectivity. But overall, less excess hydrogen is produced with higher pressure. As expected, the reduction in hydrogen production means that the methane content measured at the outlet of the low temperature WGS reactor increases as well. Another consequence of increasing pressure is the reduction in net electricity produced. This is because a higher reformer pressure also means higher bleed steam pressure from the HP turbine, resulting in less electricity production and higher compressor work. The reformer pressure sensitivity was not reduced below the base model assumption of 25 bar since the hydropyrolysis reactor pressure is 22.4 bar. Hence, accounting for pressure drops the reformer pressure cannot be appreciably lower than 25 bar without an additional compressor.

Table 17: Reformer pressure sensitivity
Values in green are base modelled case

Reformer Pressure (bar)	Excess H_2 (g/s)	CH_4 ex.LT-WGS (g/s)	Net Electricity (kW)
25	13.96	16.20	588
30	11.83	21.09	560
35	10.01	26.53	531
40	8.40	32.36	505

4.1.3. Mass and energy balance & process performance

Mass balance: Combining the mass balances from the hydropyrolysis and hydroconversion process and the Aspen Plus model for the NCG reforming, an overall system boundary mass balance was constructed as shown in Figure 8.

All water produced in the IH2 process is assumed to be treated and sent to the NCG reforming process for steam production. Further the reformation process also produces some water from the methanation of CO and CO_2, with the overall result being a surplus water stream of 0.09 kg/s, on top the 0.35 kg/s of condensed moisture removed from the as received feed. Hence the process is self-sufficient in water supply.

The char amount shown in Figure 8 is the equivalent pure carbon amount to simulate the char yield in Table 12 using the methodology explained in Section 3.1.2. Hence the actual char amount would be higher at 0.13 kg/s since the modelled pure carbon char equivalent has a higher HHV. This would mean that in actual operation the resulting flue gas flow rate would also be higher and include sulphur gas species and various ash constituents.

From the mass balance results in this section, it is now possible to calculate two performance metrics as detailed in section 3.2. The carbon recovery in HC liquid product is calculated as follows:

$$Carbon\ Recovery = \frac{Mass\ of\ Carbon\ in\ HC\ Liquid\ Product}{Mass\ of\ Carbon\ in\ Feed} = \frac{0.21 kg_{c\ in\ product}}{0.47 kg_{c\ in\ biomass\ a.f}} = 45\%$$

The HC liquid product yield can also be calculated with the mass balance results:

$$Yield_{HC\ Liquid\ Product} = \frac{Mass\ of\ HC\ Liquid\ Product}{Mass\ of\ Feed\ d.a.f.} = \frac{0.16 + 0.08}{0.94} = 26\%$$

The technology developer reports HC product liquid yields to be from 25-28% by mass, depending on the type of feed [7]. Competing fast pyrolysis and HDO upgrading processes can produce similar yields but with many more steps at different pressures, low space velocities and requiring external energy inputs either in terms of heat or hydrogen [24], [25].

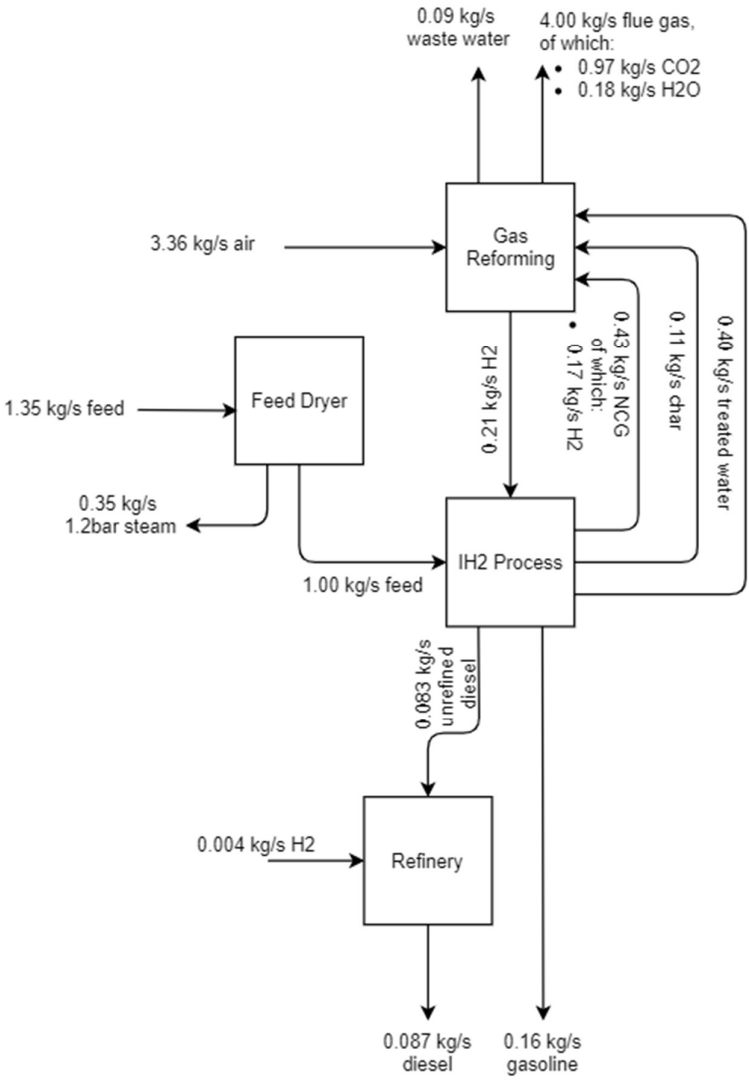

Figure 8: Overall system boundary mass balance

Energy balance: The energy balance for the IH2 process as modelled is shown in Figure 9. The heat of pyrolysis used for steam drying of the feed is shown exiting the IH2 process at 1.16 MW, which is the value assumed to be transferred to the LP pressure steam as explained in Section 3.1.3. The energetic value for NCGs going to the gas reforming process shown in Figure 9 is based on the HHV of the fraction of the gases that are sent to the furnace for combustion. Similarly, the energetic value shown for the hydrogen generated by the gas reforming process into the IH2 process is based on the HHV of the reactant hydrogen only, and not the portion of hydrogen used for fluidization and thermal regulation.

It was assumed in the mass balance that all the SMR produced hydrogen used in the refinery to upgrade the diesel product from the IH2 process was saturated into the refined diesel product. Then the energy value assigned to refined diesel was derived by multiplying the mass of the refined diesel product with the assumed HHV of refined diesel of 45.6 MJ/kg, which represents an aggregated value for diesel from different sources [63]. This compares to the unrefined diesel HHV calculated from equation 1 of 42.5 MJ/kg as per Table 13. For gasoline on the other hand, the ultimate analysis of the final product was

known and could hence be derived from equation 1, resulting in a value of 44.7 MJ/kg which is lower than typical aggregated values found in literature of around 46.9 MJ/kg [63]. But given that this gasoline is characterized as a blendstock due to some deficient qualities as per Table 5, this value seems reasonable.

From the energy balance results, it is now possible to calculate conversion efficiency and system efficiency as follows:

$$\eta_{conversion} = \frac{HC\ Liquid\ Product\ Energy}{Feedstock\ Energy} = \frac{(3.50 + 7.15)MW}{18.54MW} = 57\%$$

$$\eta_{system} = \frac{Output\ Energy}{Input\ Energy} = \frac{(3.95 + 7.15 + 0.46)MW}{(18.54 + 0.60)MW} = 60\%$$

The system efficiency is higher than the conversion efficiency for the IH2 process due to the inclusion of surplus electricity, despite the minor addition of hydrogen produced via SMR at the refinery. However, were the system to instead produce heat for services such as district heat, then this efficiency value could be even higher. Note that a detailed heat integration of the plant processes was not done in this study, for example utilization of the evaporated water as low-pressure saturated steam from feed drying. For comparison the technology developer estimates a 55% conversion efficiency[11]. This conversion efficiency is lower due to the feed having a higher assumed HHV than in this study despite similar product yields. Conversion efficiency as per Meerman & Larson [18], Jafri et. al. and Furusjö et.al. [6] were all ~60%, but this was mostly due to higher assumed liquid product yield of 27%, in addition to different HHVs attributed to the biomass feedstock, and product diesel and gasoline. System efficiency modelled by Meerman & Larson [18] was 65%. This was due to much higher electricity production rate in their Aspen Plus model (~65% more per unit biofuel produced) and assuming that the diesel product did not require any upgrading. The other three studies were incomparable in terms of system efficiency as the technology developer assumed a steam heating system instead of electricity generation while the other two studies envisioned a plant with energy integration to a pulp mill [6], [18] [49]. Hence the results from this study are conservative compared to the other studies.

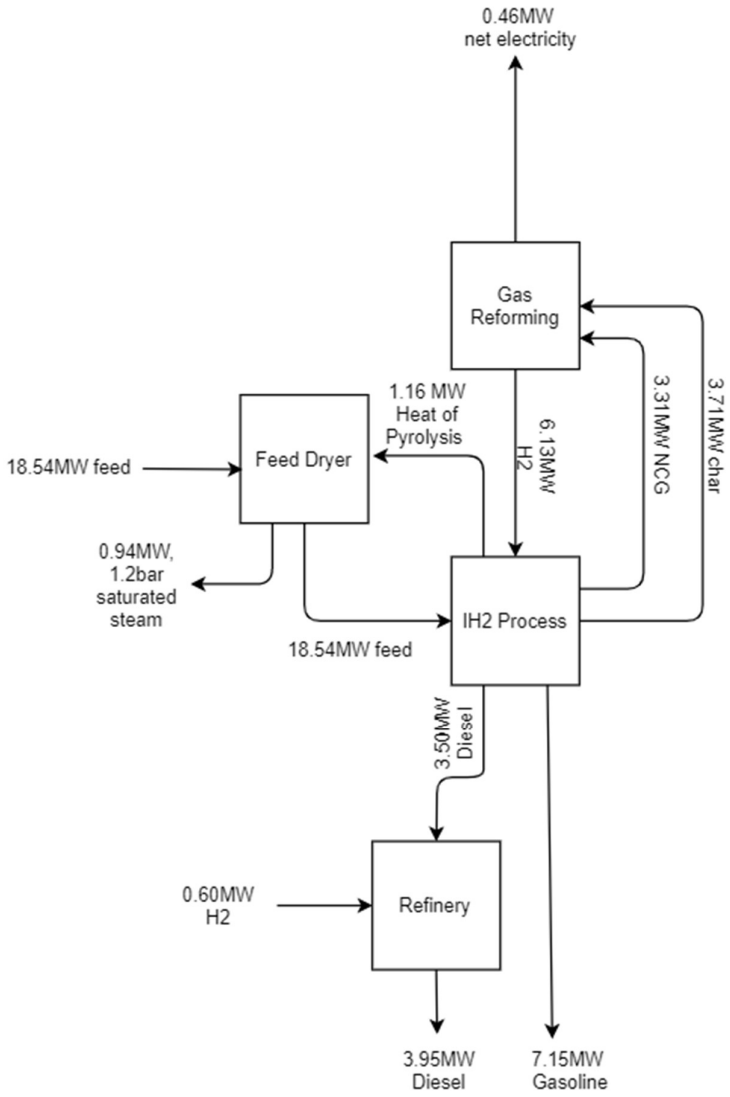

Figure 9: Overall system boundary energy balance

4.2. Economic and GHG Assessment

The results from the IH2 OPEX and GHG emissions calculations are presented in this section using energy market scenarios generated using the ENPAC tool as presented in Section 3.3.1 and the methodology described in Sections 3.3.2 and 3.3.3.

4.2.1. Economic Evaluation

The OPEX for an IH2 plant in 2030 for the SD and NP scenarios are presented in Table 18. The largest contributor to cost by a wide margin is predictably the cost of feed representing upwards of 80% and 70% of OPEX, respectively. In this study, the price of biomass is determined by the WTP of the marginal user of biomass. The marginal user is pellets for coal co-combustion and FT biofuels in the SD and NP scenarios, respectively, resulting in very different prices for the plant feedstock. In the SD scenario, the high cost of CO_2 emissions results in coal substitution, and by extension pellet production, being the driver of WTP for biomass. The NP scenario does not feature such a high charge for emissions and biofuel production is selected as the driver for biomass WTP given the large support available for biofuel producers.

Costs for upgrading the IH2 process products to diesel grade fuel at the refinery are also a large cost contributor for the IH2 process. This is due to the cost of natural gas used in the SMR process to produce hydrogen for hydroprocessing diesel at the refinery. The higher cost for refining the IH2 output diesel cut in the SD scenario compared to the NP scenario is due to the higher CO_2 emissions charge on natural gas.

Another major cost driver is the cost of electricity which provides revenue from surplus electricity sales to the grid while incurring a smaller cost for feed sizing, resulting in a net positive revenue. The surcharge for feed sizing and revenue from surplus electricity is the same across both scenarios since the build margin technology (wind) is the same. To what degree actual electricity pricing will affect costs in the future is difficult to estimate. With increasing electrification even in hard to electrify processes such as steel production, electricity usage can be expected to increase significantly, which may well lead to higher costs to cover investments in new generation and transmission capacity. For example, Northvolt's Gigafactory in Skellefteå alone is expected to consume 2.5% of Sweden's electricity output while the Hybrit fossil free steel project is projected to increase Sweden's electricity demand by 10% [64], [65].

Maintenance costs were estimated as 5% of the average of the specific TCI in Table 8, and along with labour costs represent a relatively minor part of operating expenditures as is common in upstream production facilities even in industrialized nations with higher labour costs. All other cost line items were from the technology developer's estimate [11]. The OPEX cost was not split and attributed to either bio-gasoline or bio-diesel, which are produced at a weight ratio of 66:34, because the plant cannot solely produce just one of these products. For the other three process routes, the prices for biomass, natural gas and electricity are expected to play more prominent roles depending on the process route. For example, where hydrogen is produced via SMR for HDO, the price of natural gas will be a much larger factor.

Table 18: IH2 plant specific OPEX

IH2 specific OPEX	**SD**	**NP**	**Notes**
Variable costs	**€/GJ$_{LHV\ biofuel}$**		
Feed	11.74	6.96	Assume 30% moisture in feed
Surcharge for sizing	0.31	0.31	Sized to <5mm for IH2 reactor
Bio-diesel refinery treatment	0.90	0.77	
Catalyst	0.38		[11]
Boiler operations	0.22		Make-up water & chemicals for boiler and cooling tower [11]
Gas treatment	0.04		MDEA amine solution for NH3 and H2S treatment [11]
Waste disposal	0.003		Ash and catalyst disposal [11]
WWT costs	0.03		[11]
Fixed costs			
Labour costs	0.35		Based on 62 employees for 2000T$_{biomass\ d.b}$/day plant
Overhead	0.31		90% of labour costs
Maintenance	0.12		5% of average spec annualized TCI estimated
Product credits			
Electricity export	0.58	0.58	
OPEX	**13.82**	**8.91**	

The technology developer estimated a specific OPEX of 7.10 €/GJ$_{LHV\ biofuel}$ [11]while Meerman & Larson calculated an OPEX of 10.34 €/GJ$_{LHV\ biofuel}$ for their base case scenario [18]. However,

their estimates were for plants based in the US built at the time of publishing, not in Europe in 2030 as is assumed by this study. Hence numerous differences in assumptions and policy environment are to be expected. Jafri et.al. and Furusjö et.al. reported higher OPEX values at 23 €/$GJ_{LHV\ biofuel}$ primarily due to a much higher assumed biomass feedstock price of 41 €/MWh in their 2030 scenarios, compared to 27 and 16 €/MWh assumed in this study for the SD and NP scenarios, respectively [5], [6]. Both these studies used older version of ENPAC where the biomass WTP to replace coal in the marginal power plant did not take into account various biomass transportation and processing costs which were included in the newer version of ENPAC used in this study.

Table 19 shows the ENPAC output price for bio-gasoline and bio-diesel for the SD and NP scenarios. The IH2 plant owner can expect to sell bio-diesel at the price with support if the costs for refining the bio-diesel are included in the plant OPEX as is the case in Table 18. Gasoline has no cost penalty applied as it is considered a ready blend stock as justified in Section 3.1.4 and so the producer can expect to sell the bio-gasoline product at the price with support as per Table 19. However, in reality a small penalty would likely apply for the cost incurred by the refiner to blend the IH2 bio-gasoline into a gasoline product to be sold at the pump.

The effect of the support premium for a biofuel producer is considerable and equivalent in both scenarios since the support price is set at the current levels in Sweden. It is important to note however that the biofuel price with support is not equivalent to the consumer price, rather it represents the price that a prospective biofuel producer can expect from the sale of product with subsidies. The biofuel price without support is derived in ENPAC from the consumer's WTP which is equal to the consumer price of gasoline and diesel minus the CO_2 charge, and hence represents an unsubsidized price that a producer can expect in a less supportive policy environment. The consumer price (excluding energy tax and VAT) for biofuels is then equal to the biofuel price without support plus the CO_2 charge attributable to biofuels, which is considerably lower than for fossil fuels. For this study the consumer price is not important as the primary interest is in assessing the economic viability for a prospective biofuel producer, hence only the price that the producer can expect to get at the gate is relevant.

Table 19: Biofuel sales price

Biofuel Sales Price (€/$GJ_{LHV\ biofuel}$)	**SD**	**NP**
Biofuel-Gasoline incl. support	**31.67**	**35.56**
Biofuel-Gasoline excl. support	**19.72**	**23.61**
Biofuel-Diesel incl. support	**29.44**	**33.89**
Biofuel-Diesel excl. support	**22.50**	**26.94**

Comparing then the OPEX from Table 18 against the expected selling price for the biofuel producer in Table 19, it can be seen that there is a very healthy operating margin, even without support. This would indicate that a potentially large TIC can be supported while remaining profitable. Using the assumptions in Table 9, the specific OPEX value calculated in Table 18, and using an average sales price for biofuel by weighting the biofuel price in Table 19 by its production ratio of 66:34 between gasoline and diesel, it is possible to solve for specific TCI in equation 6. The results are shown in Table 20

.

Table 20: Maximum supportable TCI

	SD		NP	
	w/suppt	w/o suppt	w/suppt	w/o suppt
Average fuel sales price (€/$GJ_{LHV\ biofuel}$)	30.91	20.67	34.99	24.74
Specific OPEX (€/$GJ_{LHV\ biofuel}$)	13.82	13.82	8.91	8.91
Max allowable spec TCI (€/$GJ_{LHV\ biofuel}$)	12.45	3.74	20.83	12.12

Table 20 confirms a large TCI is affordable while maintaining a minimum 15% specific operating margin even without support. For reference, the specific TCI for the published literature estimates from Table 8 are 3.07 €/$GJ_{LHV\ biofuel}$ for the technology developer's estimate and 1.77 €/$GJ_{LHV\ biofuel}$ for Meerman & Larson. Given that both TCI estimates in Table 8 are NOAK based estimates, the confidence in achieving a reasonable operating margin for a FOAK plant would only be questionable in the SD scenario w/o support. In all other cases the margin of safety is much larger.

4.2.2. GHG Emissions

Table 10 and the results from the previous section now allow for the calculation of a GHG emissions balance. As noted in Section 3.3.3, biogenic emission sources are not considered, land use emissions since feed is considered to come from forestry residues, and the relatively minor emissions from transportation of IH2 liquid product to the refinery and then to the consumer. The emissions balances are stated for well-to-wheel on a CO_{2eq} basis.

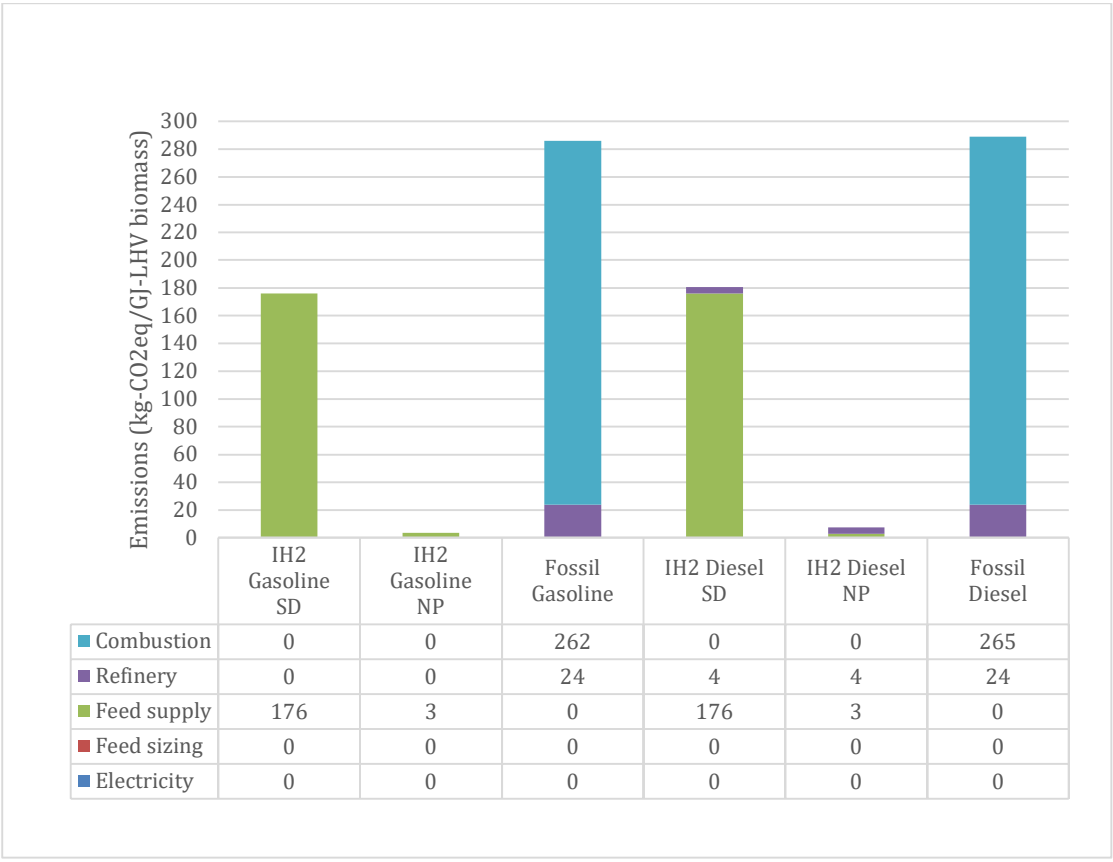

	IH2 Gasoline SD	IH2 Gasoline NP	Fossil Gasoline	IH2 Diesel SD	IH2 Diesel NP	Fossil Diesel
Combustion	0	0	262	0	0	265
Refinery	0	0	24	4	4	24
Feed supply	176	3	0	176	3	0
Feed sizing	0	0	0	0	0	0
Electricity	0	0	0	0	0	0

Figure 10: GHG emissions balance of IH2 bio-fuels vs equivalent fossil fuels

As expected, the IH2 fuel emissions are based largely on whether biomass is considered a limited resource and who the marginal user of the biomass is. In the ENPAC scenarios considered in this study, biomass is a limited resource and the marginal user is a coal fired power plant for the SD scenario, hence the high emissions attributed to the use of biomass. In the NP scenario, the marginal user is irrelevant since biomass is not considered a limited resource. The contribution of refining operations for IH2 diesel is relatively minor due to the low amounts of hydrogen required. Feed sizing and the electricity surplus do not play a role since the build margin electric power generation technology is wind in 2030 for both scenarios. If the build margin was a fossil fuel based generation technology, then the net effect would be lower emissions since the plant electricity surplus is greater than the amount of external electricity used for feed sizing, resulting in the emitting build margin plant's generation to be displaced.

In the SD scenario IH2 bio-gasoline and bio-diesel provide an emissions reduction of 38% and 39%, respectively, compared to their fossil fuel equivalents, whereas in the NP scenario the reduction is 99% and 97%, respectively. To be conservative, emissions for the transportation of the IH2 product fuels can be added to this, using a value in the range of those provided by the technology developer and Zupko between 0.6-1.25$kg_{CO2eq}/GJ_{LHV\ biofuel}$ [12], [22], but this would not greatly affect the results compared to the gains on fossil diesel and gasoline. Meerman & Larson reported a negative emissions balance of IH2 fuels (~-10$kg_{CO2eq}/GJ_{LHV\ biofuel}$) as they had a much larger electricity surplus coupled with a non-zero grid average emissions value. The technology developer estimates an emissions balance of 4.5$kg_{CO2eq}/GJ_{LHV\ biofuel}$ with the differences compared to this study owing mostly to co-product (ammonia and ammonium sulphate) credits and assuming no downstream refinery operations required for either of their gasoline nor diesel products. Jafri et.al. and Furusjö et.al. used the EU's Renewable Energy Directive (RED) guidelines to arrive at a very similar breakdown in emissions balances for IH2 fuels of around 7$kg_{CO2eq}/GJ_{LHV\ biofuel}$ split almost evenly among biomass supply and refinery operations [5], [6]. In all these studies no differentiation was made between IH2 bio-gasoline and bio-diesel products. They were instead considered as an aggregated single output stream from the plant. Zupko on the other hand made this differentiation and estimated the GHG emissions balance for IH2 bio-gasoline at between 11-15$kg_{CO2eq}/GJ_{LHV\ biofuel}$ whereas bio-diesel was at 11-16$kg_{CO2eq}/GJ_{LHV\ biofuel}$ [22]. The difference compared to this study is due mostly to the fact that Zupko considered land use effects for the emissions balance whereas ENPAC assumes no land use impact as the feed is assumed to be forestry residue.

The above analysis reveals the main drivers of emissions for the IH2 fuels, and biofuels from fast pyrolysis processes in general, and the importance of the underlying analytical assumptions. The assumptions behind the feedstock (e.g. Is the feed a limited resource? Should land use changes be considered? Who is the marginal user?) are the most important factors and should be considered carefully within the local context within which a proposed plant is to be built. Similarly, the carbon intensities of the local electricity grid supply are also very important. Sweden's electricity grid for example is largely emissions free and hence IH2 receives no credit in terms of GHG emissions balance as per the methodology in this report, although this should not be taken to mean there is no benefit since additional sources of carbon neutral electricity in a likely future with increasing electrification rates should be welcome. The emissions benefits are hence very sensitive to the assumed emissions of the build margin technology. Finally, the source and quantity of hydrogen required, either within the integrated HDO process or at the external refinery is also a major contributor to the emissions balance. For the former, there is no effect on the GHG emissions balance since the endogenous reformation process using NCGs to produce hydrogen is from a biogenic source. Likewise, for the other process routes except for where hydrogen for HDO is produced via SMR. With regards to the latter, the assumptions made on the quality of the liquid HC product at the system boundary plays a big role in determining hydrogen requirements. The other process routes will likely produce a bio-oil after HDO of a different composition and quality,

which may or may not require additional processing at a downstream refinery to become a saleable gasoline or diesel product. It should be noted that this study assumes that an external refinery facility will be using fossil fuel derived natural gas to produce hydrogen. Although this is the most common method used in refineries today, it may not be the case in 2030. Especially in a European or even Nordic context, where climate change driven policy and regulations, such as the European Green Deal, are expected to be more forceful compared to the rest of the world [66].

5. Conclusion

The Integrated Hydropyrolysis and Hydroconversion (IH2) technology for producing drop-in gasoline and diesel biofuel products from woody forest residue biomass feedstock was modelled and evaluated from a technical, economic and GHG emissions perspective. Using the technology developer's experimental data, a combination of a heat and mass balance for the main IH2 reaction process, and an Aspen Plus simulation for the NCG reforming process was developed. Some higher level assumptions were made to model the energetic requirements for the biomass drying and feed system and the exothermic heat of pyrolysis from the two IH2 reactors since more detailed information from the technology developer were not available. There is scope to further optimize the steam system and heat recovery options in the modelled plant. The wastewater treatment, flue gas treatment, Non-Condensable Gas (NCG) gas pre-treatment and co-product processing systems were not modelled as they were not deemed central to the objectives of this study.

The bio-diesel product from the IH2 process was judged to require additional hydrotreatment at an external refinery while the bio-gasoline product was judged of sufficient quality to be directly sold as a blend stock based on experimental liquid HC product characteristics.

The modelling indicated a liquid hydrocarbon yield of 26% on a d.a.f. basis and an overall system efficiency of 60%. These values are conservative compared to other published studies. The modelling also showed that the process is self-sufficient for its own internal heat and power needs, even producing a surplus of electricity, while also being able to endogenously produce all the required hydrogen for the process via NCG reforming.

The ENPAC tool was used to generate two possible future energy market scenarios used as inputs for an OPEX estimate for an IH2 plant: the Sustainable Development (SD) scenario featuring high biofuel support levels, biomass as a limited resource and a high CO_2 charge on fossil fuels; and the New Policies (NP) scenario featuring lower biofuel support levels and a lower CO_2 charge on fossil fuels. The differences between these two scenarios resulted in the biomass feedstock price being significantly higher for the SD scenario. The OPEX cost was calculated at 13.82 and 8.91 €/$GJ_{LHV\ biofuel}$ for the SD and NP scenarios, respectively, with biomass feed costs driving over 80% and 70% of OPEX costs, respectively. Final upgrading costs at a refinery and the price of wholesale electricity were a distant second and third driver of OPEX costs. The OPEX costs also allowed the calculation of the Total Capital Investment (TCI) that could be supported, which was found to be higher than previously published TCI estimates in literature. Only in the SD scenario without any biofuel support was the break-even TCI within 20% of the highest published estimates, with the other scenarios (SD with support and NP with and without support) showing break-even TCI at least 4 times higher than published estimates, indicating a potentially profitable investment opportunity.

A well-to-wheel GHG emissions balance was also conducted with the degree of emissions savings again largely dependent on the assumptions related to the biomass feed; i.e. if biomass is a limited resource, and if so, who the marginal user is. In the SD scenario, biomass was considered a limited resource with the marginal user being a coal fired power plant, hence the GHG savings were estimated to be only around 38%, while the savings were greater than

97% when biomass was not considered to be a limited resource in the NP scenario, compared to using the equivalent fossil fuel product.

Hence it can be concluded that the viability of the IH2 process largely rests on the cost of the biomass feed and the emissions associated with its use. The technology is a very promising avenue for the use of Sweden's abundant biomass resources to produce a high value-added drop-in fossil fuel substitute. As with any biofuel though, a proper evaluation of the sustainability of the fuel must also be judged in the larger context of whether the feedstock is sourced sustainably, and the wider consequences of displacing the marginal user, or opportunity costs if used in a different context.

6. Future Work

As part of the larger project to develop a techno-environmental-economic assessment of four pyrolysis-HDO integrated process routes, with a separate downstream refining step to produce drop-in transportation fuels, the results from this study, and the methodology developed within will be employed and potentially further developed to provide insights into the key differences between and drivers within the four process routes. However, there will be a few challenges to integrate the four process routes within a single comparative framework.

Firstly, within the context of process modelling, the other three process routes benefit from having an established reaction kinetic model for fast pyrolysis of biomass to reference from literature [23]. This will give a much more detailed picture of the fast pyrolysis process and the effect of different process variables on its performance compared to what was possible within this study of the IH2 process. Hence there is more scope to optimize the process whereas this study was limited by the operating conditions within the published experimental data of the technology developer. Despite this, the performance metrics used in this study should quite readily be adaptable to the other three process routes although the inter-process comparison should highlight this difference. It would also be interesting to more fully develop the steam system modelled in this study to emphasise the magnitude of the difference in energy flows in a hydropyrolysis process compared to a pyrolysis process.

The requirements for upgrading the IH2 products at an external refinery were estimated based on limited data on the characteristics of the liquid product from the IH2 process. The result was a significant impact in OPEX costs but a minor impact in terms of GHG emissions when compared to emissions from fossil fuels. Given the availability of a reaction kinetic model for the other three process streams, it will be possible to have a much clearer picture on the characteristics of the upgraded bio-oil post-HDO, and thus make a more accurate assessment on the degree of processing required from an external refinery. Here again, the inter-process comparison will be between three process routes with firmer technical grounding compared to this study.

In terms of economics, there will be numerous differences in assumptions and methodologies for the TCI and OPEX estimates between this study and other process routes. Even within this study it was not straightforward to reconcile the various estimates in published literature as each paper featured different process flowsheets and objectives (e.g. integration within a pulp mill as per Jafri et.al. and Furusjö et.al.[5], [6]), and different policy and temporal contexts within which the estimates were made. Hence the differences in assumptions that make up the estimates must be highlighted and reconciled to be able to make a meaningful comparison. The use of the ENPAC tool will ensure consistency for energy carrier pricing and substitution.

Similarly, the ENPAC tool will allow for a consistent comparison of the process routes in terms of GHG emissions. Hence it is anticipated that there should not be quite as many differences to reconcile when comparing emissions balances.

It is expected that the IH2 process will compare favourably with the other three processes given the numerous advantages of hydropyrolysis over pyrolysis as highlighted in Section 3.1.1. To what degree though will be interesting to discover in the forthcoming study. For example, the viability of the process route involving hydrogen from biomass gasification will be heavily reliant on the price and GHG emissions from biomass feed since it requires additional biomass, whereas in the process route where hydrogen is produced via electrolysis, electricity price and marginal grid emissions will be a big factor. And finally, where hydrogen is produced via SMR, the emissions and costs associated with methane will be a dominating sensitivity parameter.

References

[1] "The Climate Policy Framework," *Ministry of the Environment*, Jun. 15, 2017. https://www.government.se/articles/2017/06/the-climate-policy-framework/ (accessed Jan. 20, 2021).

[2] "SPBI Branschfakta 2019," 2019. Accessed: Mar. 24, 2021. [Online]. Available: https://drivkraftsverige.se/bestall-ladda-ner/broschyrer/spbi-branschfakta-2019/.

[3] "Roadmap Bioenergy: Meeting the Demand for Bioenergy in a Fossil Free Sweden," 2020.

[4] "ER2015:24 UP-Rapport Transportsystemet - Rådgivande underlag från utvecklingsplattform Transportsystemet till Energimyndighetens FOKUS-process," 2015.

[5] Y. Jafri, E. Wetterlund, M. Anheden, I. Kulander, Å. Håkansson, and E. Furusjö, "Multi-aspect evaluation of integrated forest-based biofuel production pathways: Part 2. economics, GHG emissions, technology maturity and production potentials," *Energy*, vol. 172, pp. 1312–1328, Apr. 2019, doi: 10.1016/j.energy.2019.02.036.

[6] E. Furusjö -, M. Anheden, I. Kulander, and J. Wallinder -RISE Bioeconomy Åsa Håkansson -Preem, "Techno-Economics of Long and Short Term Technology Pathways for Renewable Transportation Fuel Production - Detailed Report," 2018. [Online]. Available: www.f3centre.se.

[7] T. L. Marker, L. G. Felix, M. B. Linck, and M. J. Roberts, "Integrated hydropyrolysis and hydroconversion (IH 2) for the direct production of gasoline and diesel fuels or blending components from biomass, part 1: Proof of principle testing," *Environmental Progress and Sustainable Energy*, vol. 31, no. 2, pp. 191–199, Jul. 2012, doi: 10.1002/ep.10629.

[8] T. L. Marker, L. G. Felix, M. B. Linck, M. J. Roberts, P. Ortiz-Toral, and J. Wangerow, "Integrated hydropyrolysis and hydroconversion (IH2®) for the direct production of gasoline and diesel fuels or blending components from biomass, Part 2: Continuous testing," in *Environmental Progress and Sustainable Energy*, 2014, vol. 33, no. 3, pp. 762–768, doi: 10.1002/ep.11906.

[9] T. Marker *et al.*, "Long Term Processing using Integrated Hydropyrolysis plus Hydroconversion (IH 2) for the Production of Gasoline and Diesel from Biomass," 2012. [Online]. Available: www.gastechnology.org.

[10] M. Roberts *et al.*, "Biomass to Gasoline and Diesel Using Integrated Hydropyrolysis and Hydroconversion," 2010. [Online]. Available: www.gastechnology.org.

[11] E. C. D. Tan, T. L. Marker, and M. J. Roberts, "Direct production of gasoline and diesel fuels from biomass via integrated hydropyrolysis and hydroconversion

process - A techno-economic analysis," *Environmental Progress and Sustainable Energy*, vol. 33, no. 2, pp. 609–617, 2014, doi: 10.1002/ep.11791.

[12] E. Maleche, R. Glaser, T. Marker, and D. Shonnard, "A preliminary life cycle assessment of biofuels produced by the IH 2 ™ process," *Environmental Progress and Sustainable Energy*, vol. 33, no. 1, pp. 322–329, Apr. 2014, doi: 10.1002/ep.11773.

[13] D. P. Gamliel, G. M. Bollas, and J. A. Valla, "Two-stage catalytic fast hydropyrolysis of biomass for the production of drop-in biofuel," *Fuel*, vol. 216, pp. 160–170, Mar. 2018, doi: 10.1016/j.fuel.2017.12.017.

[14] V. K. Venkatakrishnan, J. C. Degenstein, A. D. Smeltz, W. N. Delgass, R. Agrawal, and F. H. Ribeiro, "High-pressure fast-pyrolysis, fast-hydropyrolysis and catalytic hydrodeoxygenation of cellulose: Production of liquid fuel from biomass," *Green Chemistry*, vol. 16, no. 2, pp. 792–802, 2014, doi: 10.1039/c3gc41558a.

[15] K. Venkatesan, F. Prashanth, V. Kaushik, H. Choudhari, D. Mehta, and R. Vinu, "Evaluation of pressure and temperature effects on hydropyrolysis of pine sawdust: Pyrolysate composition and kinetics studies," *Reaction Chemistry and Engineering*, vol. 5, no. 8, pp. 1484–1500, Aug. 2020, doi: 10.1039/d0re00121j.

[16] R. v Pindoria, A. Megaritis, A. A. Herod, and R. Kandiyoti, "A two-stage fixed-bed reactor for direct hydrotreatment of volatiles from the hydropyrolysis of biomass: effect of catalyst temperature, pressure and catalyst ageing time on product characteristics."

[17] T. van Nguyen and L. R. Clausen, "Thermodynamic analysis of polygeneration systems based on catalytic hydropyrolysis for the production of bio-oil and fuels," *Energy Conversion and Management*, vol. 171, pp. 1617–1638, Sep. 2018, doi: 10.1016/j.enconman.2018.06.024.

[18] J. C. Meerman and E. D. Larson, "Negative-carbon drop-in transport fuels produced: Via catalytic hydropyrolysis of woody biomass with CO2 capture and storage," *Sustainable Energy and Fuels*, vol. 1, no. 4, pp. 866–881, 2017, doi: 10.1039/c7se00013h.

[19] S. M. Nazir, J. H. Cloete, S. Cloete, and S. Amini, "Efficient hydrogen production with CO2 capture using gas switching reforming," *Energy*, vol. 185, pp. 372–385, Oct. 2019, doi: 10.1016/j.energy.2019.07.072.

[20] V. Spallina, D. Pandolfo, A. Battistella, M. C. Romano, M. van Sint Annaland, and F. Gallucci, "Techno-economic assessment of membrane assisted fluidized bed reactors for pure H2 production with CO2 capture," *Energy Conversion and Management*, vol. 120, pp. 257–273, Jul. 2016, doi: 10.1016/j.enconman.2016.04.073.

[21] I. Martínez, M. C. Romano, P. Chiesa, G. Grasa, and R. Murillo, "Hydrogen production through sorption enhanced steam reforming of natural gas: Thermodynamic plant assessment," *International Journal of Hydrogen Energy*, vol. 38, no. 35, pp. 15180–15199, Nov. 2013, doi: 10.1016/j.ijhydene.2013.09.062.

[22] R. Zupko, "Life cycle assessment of the production of gasoline and diesel from forest residues using integrated hydropyrolysis and hydroconversion," *International Journal of Life Cycle Assessment*, vol. 24, no. 10, pp. 1793–1804, Oct. 2019, doi: 10.1007/s11367-019-01616-8.

[23] M. B. Gorensek, R. Shukre, and C. C. Chen, "Development of a Thermophysical Properties Model for Flowsheet Simulation of Biomass Pyrolysis Processes," *ACS Sustainable Chemistry and Engineering*, vol. 7, no. 9, pp. 9017–9027, May 2019, doi: 10.1021/acssuschemeng.9b01278.

[24] E. F. Iliopoulou, K. S. Triantafyllidis, and A. A. Lappas, "Overview of catalytic upgrading of biomass pyrolysis vapors toward the production of fuels and high-value chemicals," *Wiley Interdisciplinary Reviews: Energy and Environment*, vol. 8, no. 1, p., Jan. 2019, doi: 10.1002/wene.322.

[25] E. Kantarelis, W. Yang, and W. Blasiak, *Technologies for Converting Biomass to Useful Energy: combustion, gasification, pyrolysis, torrefaction and fermentation; Chapter 8*, 1st ed. CRC Press, 2013.
[26] D. C. Elliott, "Historical Developments in Hydroprocessing Bio-oils," *Energy & Fuels*, vol. 21, no. 3, May 2007, doi: 10.1021/ef070044u.
[27] Q. Zhang, J. Chang, T. Wang, and Y. Xu, "Review of biomass pyrolysis oil properties and upgrading research," *Energy Conversion and Management*, vol. 48, no. 1, Jan. 2007, doi: 10.1016/j.enconman.2006.05.010.
[28] A. P. Pinheiro Pires *et al.*, "Challenges and Opportunities for Bio-oil Refining: A Review," *Energy & Fuels*, vol. 33, no. 6, Jun. 2019, doi: 10.1021/acs.energyfuels.9b00039.
[29] "Integrated Hydropyrolysis & Hydroconversion." https://www.shell.com/business-customers/catalysts-technologies/licensed-technologies/benefits-of-biofuels/ih2-technology/hydropyrolysis.html (accessed Jan. 12, 2021).
[30] "$2.25 per gallon biohydrocarbon fuels, unsubsidized? Biozin licenses IH2 Technology — heads for commercial-scale in Norway," *Biofuels Digest*, Nov. 15, 2017. https://www.biofuelsdigest.com/bdigest/2017/11/15/2-25-per-gallon-biohydrocarbon-fuels-unsubsidized-biozin-licenses-ih2-technology-heads-for-commercial-scale-in-norway/ (accessed Jan. 24, 2021).
[31] M. Linck, L. Felix, T. Marker, and M. Roberts, "Integrated biomass hydropyrolysis and hydrotreating: A brief review," *Wiley Interdisciplinary Reviews: Energy and Environment*, vol. 3, no. 6, pp. 575–581, Nov. 2014, doi: 10.1002/wene.119.
[32] Shell Oil Company, "Conversion of Biomass or Residual Waste Material to Biofuels," US 2017/0009143 A1, Jan. 12, 2017.
[33] T. Marker, L. Felix, and M. Linck, "Hydropyrolysis of biomass for producing high quality fuels," US 8.492,600 B2, Jun. 23, 2013.
[34] D. Mehta, V. Urade, L. Narasimhan, M. Rao, and A. del Paggio, "Understanding Chemistry in the IH2® Process ," 2015.
[35] D. Kunii and O. Levenspiel, *Fluidization Engineering*, 2nd ed. Butterworth-Heinemann, 1991.
[36] S. A. Channiwala and P. P. Parikh, "A unified correlation for estimating HHV of solid, liquid and gaseous fuels," *Fuel*, vol. 81, no. 8, May 2002, doi: 10.1016/S0016-2361(01)00131-4.
[37] M. Ryden and A. Lyngfel, "Using steam reforming to produce hydrogen with carbon dioxide capture by chemical-looping combustion," *International Journal of Hydrogen Energy*, vol. 31, no. 10, Aug. 2006, doi: 10.1016/j.ijhydene.2005.12.003.
[38] P. Nikolaidis and A. Poullikkas, "A comparative overview of hydrogen production processes," *Renewable and Sustainable Energy Reviews*, vol. 67, Jan. 2017, doi: 10.1016/j.rser.2016.09.044.
[39] R. Elshout, "Hydrogen Production by Steam Reforming," *Chemical Engineering*, pp. 34–38, May 2010.
[40] M. Moran and H. Shaprio, *Fundamentals of Engineering Thermodynamics*, 4th ed. John Wiley & Sons Inc. , 2000.
[41] T. Marker, M. Roberts, J. Wangerow, P. Ortiz-Toral, M. Linck, and D. Swanson, "Biomass to Gasoline and Diesel using IH2® Key Pilot Plant Tests on the Road to Commercialization," Mar. 2010.
[42] A. G. McDonald, J. S. Gifford, D. Steward, P. H. Dare, S. Riley, and I. Simpson, "Air emission from timber drying: high temperature drying and re-drying of CCA treated timber," *Holz als Roh- und Werkstoff*, vol. 62, no. 4, Aug. 2004, doi: 10.1007/s00107-004-0494-x.
[43] H. Li, Q. Chen, X. Zhang, K. N. Finney, V. N. Sharifi, and J. Swithenbank, "Evaluation of a biomass drying process using waste heat from process

industries: A case study," *Applied Thermal Engineering*, vol. 35, Mar. 2012, doi: 10.1016/j.applthermaleng.2011.10.009.
[44] A. Alamia, H. Ström, and H. Thunman, "Design of an integrated dryer and conveyor belt for woody biofuels," *Biomass and Bioenergy*, vol. 77, Jun. 2015, doi: 10.1016/j.biombioe.2015.03.022.
[45] J. Dai, H. Cui, and J. R. Grace, "Biomass feeding for thermochemical reactors," *Progress in Energy and Combustion Science*, vol. 38, no. 5, Oct. 2012, doi: 10.1016/j.pecs.2012.04.002.
[46] N. S. Osborne and D. C. Ginnings, "Measurements of Heat of Vaporization and Heat Capac-ity of a Number of Hydrocarbons."
[47] TransportPolicy.net, "EU Fuels: Diesel & Gasoline." https://www.transportpolicy.net/standard/eu-fuels-diesel-and-gasoline/ (accessed Apr. 24, 2021).
[48] "Worldwide Fuel Charter for Gasoline and Diesel Fuel," Oct. 2019.
[49] Y. Jafri, E. Wetterlund, M. Anheden, I. Kulander, Å. Håkansson, and E. Furusjö, "Multi-aspect evaluation of integrated forest-based biofuel production pathways: Part 1. Product yields & energetic performance," *Energy*, vol. 166, pp. 401–413, Jan. 2019, doi: 10.1016/j.energy.2018.10.008.
[50] "Energy balance guide: Methodology guide for the construction of energy balances & Operational guide for the energy balance builder tool," Jan. 2019.
[51] K. Isaac and S. O. Bada, "The co-combustion performance and reaction kinetics of refuse derived fuels with South African high ash coal," *Heliyon*, vol. 6, no. 1, Jan. 2020, doi: 10.1016/j.heliyon.2020.e03309.
[52] E. Axelsson and K. Pettersson, "Energy price and Carbon Balances Scenarios tool (ENPAC) – a summary of recent updates ," Göteborg, 2014.
[53] E. Axelsson and S. Harvey, "Scenarios for assessing profitability and carbon balances of energy investments in industry, AGS Pathways report 2010:EU1," Göteborg, 2010.
[54] E. Axelsson, M. Bisaillon, and E. Löfblad, "ENPAC 2.1 – update of the wood fuel module," Göteborg, 2018.
[55] "World Energy Outlook 2017," Paris, 2017.
[56] C. Acar and I. Dincer, "Review and evaluation of hydrogen production options for better environment," *Journal of Cleaner Production*, vol. 218, May 2019, doi: 10.1016/j.jclepro.2019.02.046.
[57] J. Wang, J. Gao, K. L. Brandt, and M. P. Wolcott, "Energy consumption of two-stage fine grinding of Douglas-fir wood," *Journal of Wood Science*, vol. 64, no. 4, Aug. 2018, doi: 10.1007/s10086-018-1712-1.
[58] "The Chemical Engineering Plant Cost Index." https://www.chemengonline.com/pci-home (accessed May 09, 2021).
[59] "Årsgenomsnitt valutakurser (ackumulerat)." https://www.riksbank.se/sv/statistik/sok-rantor--valutakurser/arsgenomsnitt-valutakurser/ (accessed May 09, 2021).
[60] D. Pham Minh *et al.*, "Hydrogen Production From Biogas Reforming: An Overview of Steam Reforming, Dry Reforming, Dual Reforming, and Tri-Reforming of Methane," in *Hydrogen Supply Chains*, Elsevier, 2018.
[61] A. Blasi, G. Fiorenza, C. Freda, and V. Calabrò, "Steam reforming of biofuels for the production of hydrogen-rich gas," in *Membranes for Clean and Renewable Power Applications*, Elsevier, 2014.
[62] M. Z. Hossain and P. A. Charpentier, "Hydrogen production by gasification of biomass and opportunity fuels," in *Compendium of Hydrogen Energy*, Elsevier, 2015.
[63] I. Staffell, "The Energy and Fuel Data Sheet," *University of Birmingham*, 2011. https://www.claverton-energy.com/wordpress/wp-content/uploads/2012/08/the_energy_and_fuel_data_sheet1.pdf (accessed May 16, 2021).

[64] “100 percent renewable electricity by 2040: wind power combating climate change and improving competitiveness,” 2019.
[65] O. Olsson and B. Nykvist, “Bigger is sometimes better: demonstrating hydrogen steelmaking at scale ,” 2020.
[66] “In focus: Hydrogen – driving the green revolution.” https://ec.europa.eu/info/news/focus-hydrogen-driving-green-revolution-2021-abr-14_en (accessed May 03, 2021).
[67] “Gas Viscosity Caculator.” https://www.lmnoeng.com/Flow/GasViscosity.php (accessed Apr. 05, 2021).
[68] C. Dupont, R. Chiriac, G. Gauthier, and F. Toche, “Heat capacity measurements of various biomass types and pyrolysis residues,” *Fuel*, vol. 115, Jan. 2014, doi: 10.1016/j.fuel.2013.07.086.
[69] “Thermophysical Properties of Fluid Systems,” *National Instiure of Standards and Technology*. https://nordaccount.com/error?challenge=a63de6db89b84170ad2d366e74716fff&code=400&ref=%2Faccount%2Fselect&type=session_expired (accessed Mar. 03, 2021).

Appendix A - H2 Flow Rate Calculation for Hydropyrolysis

H2 as a fluidizing agent: The amount of hydrogen required to fluidize the hydropyrolysis reactor bed, where the catalyst is the fluidizing medium, is calculated using the equations below.

It is assumed that the amount of hydrogen required for fluidizing the catalyst bed is the more or less the same amount as required to fluidize the catalyst bed with the biomass feed as the feed amount at any given time in the bed is small compared to the mass of the catalyst.

Parameter	Description	Value	Source
d_c (m)	Average particle size	$300x10^{-6}$	[18]
ρ_c (kg/m^3)	Catalyst particle density	1500	
ρ_b (kg/m^3)	Bed bulk density at rest	1000	
Δp_R (Bar)	Reactor pressure drop	0.5	
μ_{H2} (kg/m/s)	H_2 dynamic viscosity in reactor	$1.48x10^{-5}$	[67]
ρ_{H2} (kg/ m^3)	Density of H_2 at 22.4bar	1.72	Aspen Plus
WHSV (kg_{fd}/kg_{cat}/h)	Hydropyrolysis WHSV	1.62	[7]
$\dot{m}_{feed}$(kg/s)	Feed rate	1.0	

The calculations for fluidizing hydrogen amount hinges on the WHSV as reported by the technology developer. The formulas used below are from literature [18], [35].

Bed catalyst weight

$$W = \frac{\dot{m}_{feed} * 3600}{WHSV} = 2222\ kg$$

Bed volume at rest

$$V_b = \frac{W}{\rho_b} = 2.22\ m^3$$

Bed cross sectional area, resulting in bed diameter of 0.75m, and a reactor height 5.10m for a plant at this feed rate

$$A_b = \frac{W * g}{\Delta p_B} = 0.44\ m^2$$

Archimedes number

$$Ar = \frac{d_c^3 * \rho_{H2} * (\rho_c - \rho_{H2}) * g}{\mu_{H2}^2} = 3124$$

Minimum fluidization velocity

$$v_{f,min} = \frac{Ar * \mu_{H2}}{1502 * d_c * \rho_{H2}} = 0.06 \frac{m}{s}$$

Design fluidization velocity, $v_{f,des}$ to be double the minimum fluidization velocity. Then hydrogen fluidization rate is:

$$\dot{m}_{H2} = v_{f,des} * A_b * \rho_{H2} = 0.09 \frac{kg}{s}$$

Reactant hydrogen rate of 0.04kg/s is added on to this, resulting in a value of 0.13kg/s of hydrogen per kg/s of a.f. biomass, or **0.14kg_{H2}/$kg_{biomass\ d.a.f.}$**

H2 as a thermal regulator: Since the hydropyrolysis process is exothermic, sufficient hydrogen is required to keep the process temperature of pyrolysis products exiting the reactor at 389°C. Ambient temperature is assumed to be 25°C with biomass feed entering the reactor at 104°C which is the saturation temperature of low-pressure drying steam, while hydrogen enters the reactor from the reformer at 41°C as per Aspen model. This value is calculated by completing an energy balance around the combined control volume of the hydropyrolysis and hydroconversion reactors where the only unknown is the hydrogen flow rate. The heat of combustion (ΔH_c) is used to estimate chemical energy that is in turn assumed to heat up the pyrolysis products. The hydropyrolysis reactor is assumed to be adiabatic.

The inputs to the energy balance are as per mass balance in Table 11 and the table below

Parameter	Value	Source
$C_{p,biomass}$ (kJ/kg/K)	1.35	[68], assumed constant from 25-104 °C
$C_{p,H2}$ (kJ/kg/K)	14.71	[69], assumed constant from 41-389 °C at 22.4 bar
$C_{p,\ char}$ (kJ/kg/K)	1.80	[18], assumed constant from 25-104 °C
$C_{p,condensable\ HC}$ (kJ/kg/K)	2.00	[18], assumed constant from 104-389 °C
$\Delta H_{c,\ biomass\ d.b.}$(MJ/kg)	19.64	[36], as per equation 1
$\Delta H_{c,\ char.}$(MJ/kg)	28.39	[36], as per equation 1
$\Delta H_{c,\ H2}$(MJ/kg)	141.78	[40]
$\Delta H_{c,\ CO}$(MJ/kg)	10.10	[40]
$\Delta H_{c,\ CH4}$(MJ/kg)	55.51	[40]
$\Delta H_{c,\ C2H6}$(MJ/kg)	51.87	[40]
$\Delta H_{c,\ C3H8}$(MJ/kg)	50.35	[40]
$\Delta H_{c,\ condensable\ HC}$ (MJ/kg)	44.16	[36], as per equation 1
$\Delta E_{therm,H2O+NCG}$	2.20	Aspen Plus, from 25-389 °C

The following equation is used to calculate thermal energy:

$$Thermal\ Energy\ (MW) = \sum \left(\dot{m}_i * c_p * \Delta T\right)$$

Hence, thermal energy of incoming biomass:

$$E_{T,biomass} = 1\frac{kg}{s} * 1.35\frac{kJ}{kgK} * (104 - 25)K = 0.11MW$$

Thermal energy of incoming reactant hydrogen:

$$E_{T,reactant\ H2} = 0.04\frac{kg}{s} * 14.71\frac{kJ}{kgK} * (41 - 25)K = 0.01MW$$

Thermal energy of outgoing water and NCG (excluding hydrogen):

$$E_{T,NCG+H2O} = 0.67\frac{kg}{s} * 2.20\frac{MJ}{kg} = 1.48MW$$

Thermal energy of outgoing char:

$$E_{T,char} = 0.13\frac{kg}{s} * 1.80\frac{kJ}{kgK} * (389 - 25)K = 0.09MW$$

Thermal energy of outgoing HC liquid:

$$E_{T,condensable\ HC} = 0.24\frac{kg}{s} * 2.00\frac{kJ}{kgK} * (389 - 25)K = 0.18MW$$

Using equation 3 to calculate chemical energy

$$Chemical\ Energy\ (MW) = \sum(\dot{m}_i * \Delta H_c)$$

Hence chemical energy released by biomass, excluding moisture content:

$$E_{C,biomass} = 0.94\frac{kg}{s} * 19.64\frac{MJ}{kg} = 18.54MW$$

Chemical energy released by reactant hydrogen:

$$E_{C,reactant\ H2} = 0.04\frac{kg}{s} * 141.78\frac{MJ}{kg} = 6.13MW$$

Chemical energy of NCGs:

$$E_{C,NCG} = 0.06\frac{kg}{s} * 10.10\frac{MJ}{kg} + 0.04\frac{kg}{s} * 55.51\frac{MJ}{kg} + 0.06\frac{kg}{s} * 51.87\frac{MJ}{kg} + 0.04\frac{kg}{s} * 50.35\frac{MJ}{kg} = 7.75MW$$

Chemical energy of Char:

$$E_{C,char} = 0.13\frac{kg}{s} * 28.39\frac{MJ}{kg} = 3.71MW$$

Chemical energy of HC liquid:

$$E_{C,condensable\ HC} = 0.24\frac{kg}{s} * 44.16\frac{MJ}{kg} = 10.70MW$$

Finally, hydrogen required for thermal regulation, $\dot{m}_{H2,TR}$ is solved whereby energy of inputs equals energy of outputs:

$$E_{T,biomass} + E_{T,reactant\ H2} + E_{C,biomass} + E_{C,reactant\ H2} = E_{T,NCG+H} + E_{T,char} + E_{T,condensable\ HC} + E_{C,NCG} + E_{C,char} + E_{C,condensable\ HC} + \dot{m}_{H2,TR} * c_{p,H2} * (389 - 25)$$

Solving for thermal regulation hydrogen flow rate

$$\dot{m}_{H2,TR} = 0.17kg/s$$

Reactant hydrogen rate of 0.04kg/s is added on to this, resulting in a value of 0.21kg/s of hydrogen per kg/s of a.f. biomass, or **0.22kg$_{H2}$/kg$_{biomass\ d.a.f.}$**

Appendix B – Heating Values

The table below shows the heating values used in this study and the source from which they were obtained.

Energy carrier	LHV (MJ/kg)	HHV (MJ/kg)	Notes
Biomass a.r.	12.12	13.75	HHV derived as per equation 1, from [36] LHV derived as per equation 3, from [51]
Biomass a.f.	17.19	18.54	
Biomass d.b.	19.64	19.64	
Char	28.00	28.39	
Pure carbon	-	32.77	Used to simulate char [40]
IH2 bio-gasoline blendstock	41.98	44.70	HHV derived as per equation 1, from [36] LHV derived as per equation 3, from [51]
IH2 unrefined bio-diesel	40.37	42.50	
IH2 refined bio-diesel	43.00	45.60	HHV from [63], LHV from [50]

Appendix C – Currency Conversion and Cost Indexes

Year	Annual average exchange rates[59]		
	SEK/USD	SEK/€	€/USD
1991	6.16	7.45	0.83
1992	5.81	7.52	0.77
1993	7.80	9.10	0.86
1994	7.71	9.14	0.84
1995	7.13	9.23	0.77
1996	6.70	8.40	0.80
1997	7.64	8.62	0.89
1998	7.95	8.93	0.89
1999	8.27	8.81	0.94
2000	9.17	8.45	1.09
2001	10.33	9.25	1.12
2002	9.72	9.16	1.06
2003	8.09	9.12	0.89
2004	7.35	9.13	0.81
2005	7.48	9.28	0.81
2006	7.38	9.25	0.80
2007	6.76	9.25	0.73
2008	6.58	9.61	0.68
2009	7.65	10.62	0.72
2010	7.20	9.54	0.76
2011	6.50	9.03	0.72
2012	6.78	8.71	0.78
2013	6.51	8.65	0.75
2014	6.86	9.10	0.75
2015	8.40	9.37	0.90
2016	8.56	9.47	0.90
2017	8.54	9.63	0.89
2018	8.69	10.26	0.85
2019	9.46	10.59	0.89
2020	9.20	10.49	0.88

Year	CEPCI Index [58]	
	Composite	Labour
2000	394	299
2001	394	302
2002	396	306
2003	402	309
2004	444	308
2005	468	306
2006	500	309
2007	525	315
2008	575	322
2009	522	327
2010	551	329
2011	586	327
2012	585	323
2013	567	320
2014	576	321
2015	557	322
2016	542	325
2017	535	328
2018	603	335
2019	608	336
2020	596	336

The two tables above represent the currency conversion rates from Sweden's Riksbanken [59] and the CEPCI index [58]used in calculating 2019 prices for TCI and OPEX estimates as per equation 4 & 5 .

Appendix D – NCG Reforming Process Data

Relevant gas stream process data from the NCG reforming Aspen Plus model is shown below.

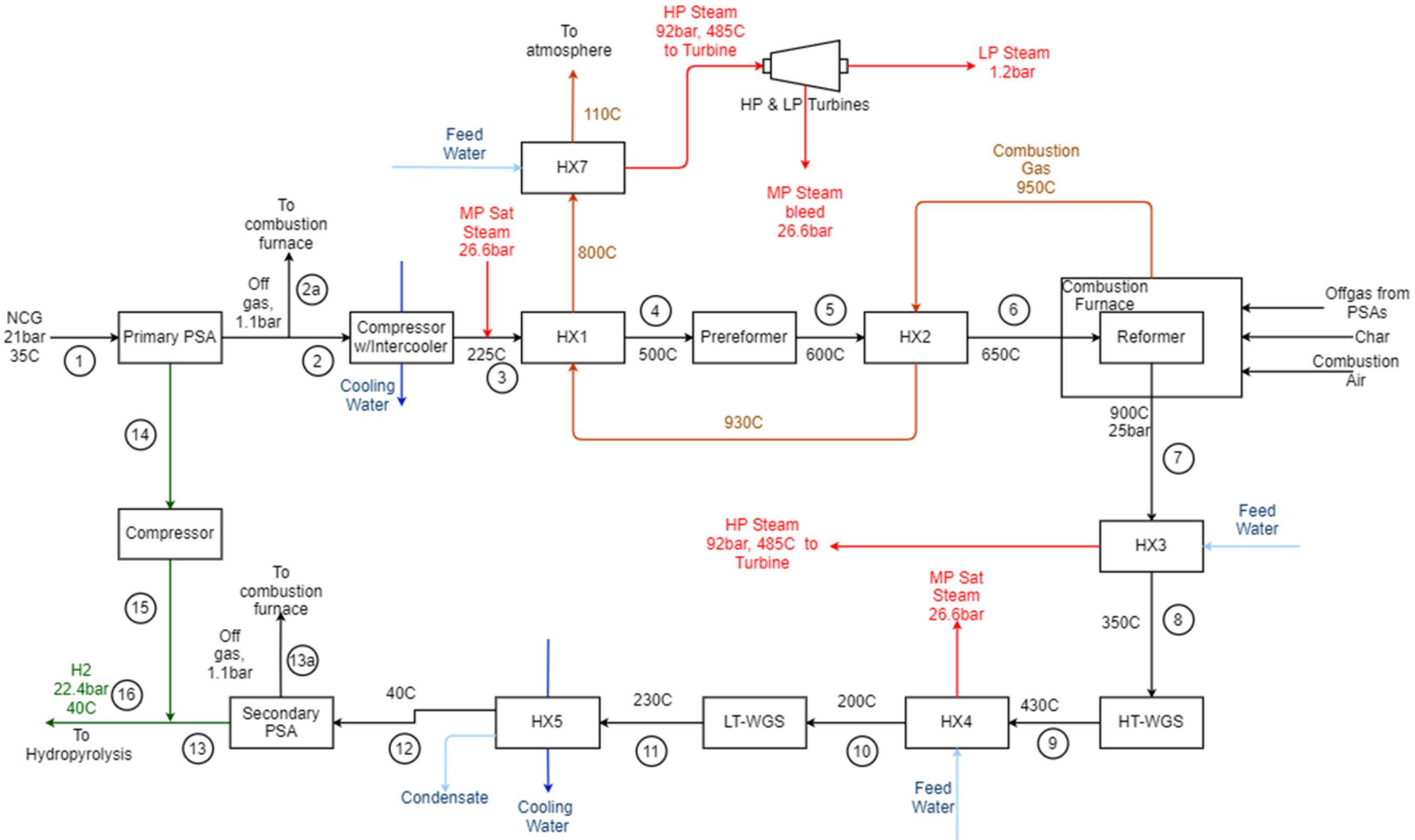

The process points shown in the table correspond to the numbering on the process flow diagram below. Figure 7 in the main body of the reportis based off this table.

		1	2	2A	3	4	5	6	7	8	9	10	11	12	13	13A	14	15	16
Temperature	C	35	31	31	208	500	607	650	900	350	429	200	230	35	36	21	35	43	40
Pressure	bar	21.0	1.1	1.1	26.6	26.0	25.8	25.3	25.0	24.5	24.3	23.8	23.5	23.1	22.4	1.1	20.8	22.4	22.4
Total	kg/sec	0.432	0.280	0.014	0.900	0.900	0.900	0.900	0.900	0.900	0.900	0.900	0.900	0.587	0.070	0.517	0.138	0.138	0.208
H2	kg/sec	0.165	0.026	0.001	0.026	0.026	0.024	0.024	0.069	0.069	0.079	0.079	0.083	0.083	0.070	0.013	0.138	0.138	0.208
H20	kg/sec	0	0	0	0.620	0.620	0.581	0.581	0.439	0.439	0.347	0.347	0.315	0.002	0	0.002	0	0	0
CO2	kg/sec	0.070	0.066	0.003	0.066	0.066	0.149	0.149	0.176	0.176	0.400	0.400	0.480	0.480	0	0.480	0	0	0
CO	kg/sec	0.061	0.058	0.003	0.058	0.058	0.014	0.014	0.199	0.199	0.057	0.057	0.006	0.006	0	0.006	0	0	0
CH4	kg/sec	0.035	0.033	0.002	0.033	0.033	0.132	0.132	0.016	0.016	0.016	0.016	0.016	0.016	0	0.016	0	0	0
C2H6	kg/sec	0.063	0.060	0.003	0.060	0.060	0	0	0	0	0	0	0	0	0	0	0	0	0
C3H8	kg/sec	0.038	0.037	0.002	0.037	0.037	0	0	0	0	0	0	0	0	0	0	0	0	0

DEPARTMENT OF SPACE, EARTH & ENVIRONMENT
CHALMERS UNIVERSITY OF TECHNOLOGY
Gothenburg, Sweden 2021
www.chalmers.se

CHALMERS
UNIVERSITY OF TECHNOLOGY